

# 山西繁峙新生代玄武岩地幔源区及成因探讨:元素及 Sr-Nd-Pb-Hf 同位素地球化学证据\*

叶蕾<sup>1</sup> 刘金菊<sup>1</sup> 牛耀龄<sup>2,3\*\*</sup> 郭鹏远<sup>1</sup> 孙普<sup>1</sup> 崔慧霞<sup>1</sup>

YE Lei<sup>1</sup>, LIU JinJu<sup>1</sup>, NIU YaoLing<sup>2,3\*\*</sup>, GUO PengYuan<sup>1</sup>, SUN Pu<sup>1</sup> and CUI HuiXia<sup>1</sup>

1. 兰州大学地质科学与矿产资源学院,兰州 730000

2. Department of Earth Science, Durham University, Durham DH1 3LE, UK

3. 中国科学院海洋研究所海洋地质与环境重点实验室,青岛 266071

1. School of Earth Sciences, Lanzhou University, Lanzhou 730000, China

2. Department of Earth Sciences, Durham University, Durham DH1 3LE, UK

3. Key Laboratory of Marine Geology and Environment, Institute of Oceanology, Chinese Academy of Sciences, Qingdao 266071, China

2013-10-23 收稿, 2014-09-02 改回.

Ye L, Liu JJ, Niu YL, Guo PY, Sun P and Cui HX. 2015. Mantle sources and petrogenesis of the Cenozoic basalts in Fanshi, Shanxi Province: Geochemical and Sr-Nd-Pb-Hf isotopic evidence. *Acta Petrologica Sinica*, 31(1):161–175

**Abstract** The Fanshi basalts located in the vicinity of the Da Hinggan Ling-Taihangshan gravity gradient zone, represent a major component of Cenozoic basalts of the central North China Craton. Previous studies gave the Fanshi basalts whole rock K-Ar ages of 26.3 ~ 24.3 Ma. The Fanshi basalts from Sumengzhuang and Yingxian two locations all show OIB-like trace element and isotopic signatures, i. e., they are enriched in incompatible elements with highly fractionated LREEs and HREEs ( $(La/Yb)_N = 8.42 \sim 21.60$ ) without negative Sr and Eu anomalies. They show relatively low Sr ( $^{87}Sr/^{86}Sr = 0.703848 \sim 0.704870$ ) and high Nd ( $^{143}Nd/^{144}Nd = 0.512617 \sim 0.513057$ ), Hf ( $^{176}Hf/^{177}Hf = 0.282873 \sim 0.283001$ ) isotope ratios, and Pb isotope ratios were  $^{206}Pb/^{204}Pb = 17.2 \sim 17.9$ ,  $^{207}Pb/^{204}Pb = 15.3 \sim 15.4$  and  $^{208}Pb/^{204}Pb = 37.5 \sim 37.9$ . All these geochemical features, combined with petrographic observations and major element data, allow us to suggest that the Fanshi basalts were derived from small degree partial melting of asthenospheric mantle with contributions of metasomatized lithospheric mantle. Olivine and clinopyroxene dominated fractional crystallization is an important process in the petrogenesis of these basalts, which may have taken place in magma chamber of lithospheric mantle condition. The rapid ascent explains the lack of crustal contamination. Sumengzhuang samples are characterized by relatively deeper and lower extent of melting, whereas the Yingxian samples have the signature of slightly shallower and higher extent of melting. Together with studies of Cenozoic basalts in other areas near the gravity gradient zone, we suggest that the Cenozoic basalts near the Gravity Gradient zone may be originated from decompression melting of eastward asthenosphere flow when crossing the gravity gradient zone. This study offers some new perspectives on the petrogenesis of the Cenozoic basaltic volcanism in eastern China in general.

**Key words** Cenozoic basalts; Gravity gradient zone; Geochemistry; Formation mechanism; Fanshi region; North China Craton

**摘要** 山西省繁峙玄武岩位于华北克拉通重力梯度带附近,是华北克拉通中部新生代玄武岩重要组成部分。前人全岩 K-Ar 测年结果为 26.3 ~ 24.3 Ma。对繁峙地区苏孟庄和应县两地玄武岩的地球化学特征研究表明,其微量元素和同位素均具有类 OIB 特征,即富集不相容元素,轻、重稀土元素分馏明显( $(La/Yb)_N = 8.42 \sim 21.60$ ),不存在 Sr、Eu 负异常, Sr 同位素比值 ( $^{87}Sr/^{86}Sr = 0.703848 \sim 0.704870$ ) 较低, Nd ( $^{143}Nd/^{144}Nd = 0.512617 \sim 0.513057$ ) 和 Hf ( $^{176}Hf/^{177}Hf = 0.282873 \sim 0.283001$ ) 同位素比值较高, Pb 同位素比值分别为  $^{206}Pb/^{204}Pb = 17.2 \sim 17.9$ ,  $^{207}Pb/^{204}Pb = 15.3 \sim 15.4$  和  $^{208}Pb/^{204}Pb = 37.5 \sim 37.9$ 。结合岩相学特征和主量元素特征,我们推断繁峙新生代玄武岩是软流圈低程度部分熔融结果,并存在岩石圈物质的加入,岩浆上升

\* 本文受国家自然科学基金项目(91014003,41130314)资助。

第一作者简介:叶蕾,1990年生,女,硕士,主要从事岩石地球化学方面的研究,E-mail: ye08@lzu.edu.cn

\*\* 通讯作者:牛耀龄,男,1959年生,教授,岩石地球化学专业,E-mail: yaoling.niu@foxmail.com

时在岩石圈地幔条件下的岩浆房内经历了以橄榄石、单斜辉石为主的分离结晶作用,岩浆因快速上升而地壳混染程度甚低。苏孟庄碱性玄武岩具有较深的熔融深度和较低的熔融程度,而应县亚碱性玄武岩熔融深度较浅,熔融程度较高。结合重力梯度带附近其他地区的新生代玄武岩的研究,我们推测重力梯度带附近新生代的火山活动可能起源于西部软流圈地幔向东流动越过重力梯度带时的减压部分熔融,该地区广泛分布的断裂带为岩浆上涌提供了通道。本文为中国东部新生代玄武质火山活动的岩石成因学研究提供了新的视角。

**关键词** 新生代玄武岩;重力梯度带;地球化学;形成机制;繁峙;华北

**中图法分类号** P588.145

玄武岩是地幔岩部分熔融的产物,其化学组成和同位素组成受控于地幔源区、部分熔融程度、地幔潜在温度和岩石圈厚度等诸多因素,因此可用于反演深部地幔的演化历史,是人类认识地球深部的重要窗口(Niu and Batiza, 1991; Niu *et al.*, 1996, 2001, 2011; Langmuir *et al.*, 1992; Depaolo and Daley, 2000; 徐义刚, 2006b)。华北克拉通广泛分布的中、新生代板内玄武岩为研究该地区深部地幔的性质和演化提供了天然样品。

华北克拉通东西两侧(以大兴安岭-太行山重力梯度带为界)玄武岩的时空分布存在较大的差异。东部的中、新生代玄武岩分布较广,前人研究较多(Deng *et al.*, 1998, 2004; 徐义刚, 1999; Xu, 2001; Zheng *et al.*, 2001, 2007; Zhang *et al.*, 2002; Wu *et al.*, 2003, 2006; Gao *et al.*, 2004; Xu *et al.*, 2006, 2009, 2010),而重力梯度带以西的地区,除了汉诺坝因含有丰富的幔源包体,研究程度较高以外(Fan and Hopper, 1991; Basu *et al.*, 1991; Song *et al.*, 1990; Zhi *et al.*, 1990; Choi *et al.*, 2008; Zheng *et al.*, 2009),其他地区的玄武岩直到最近几年才被重视(马金龙和徐义刚, 2004; Xu *et al.*, 2005; Tang *et al.*, 2006; Ho *et al.*, 2011; Zhang *et al.*, 2012a, b; 朱昱升等, 2012)。且西部玄武岩主要分布在重力梯度带附近,根据前人的 K-Ar 定年结果,主要属于新生代玄武岩(王慧芬等, 1988; 刘若新等, 1992; Tang *et al.*, 2006),我们推测这种时空特殊性对其成因应该有某种指示意义。

华北克拉通是世界上最古老的陆核之一,但是与全球大多克拉通不同的是,华北克拉通岩石圈发生了较大程度的减薄(Menzies *et al.*, 1993; Griffin *et al.*, 1998, 1999, 2003; Fan *et al.*, 2000; Xu, 2001; Zheng *et al.*, 2001),从古生代的 200km 减薄到了新生代的 <90km(Fan and Menzies, 1992; Zheng *et al.*, 2009)。华北克拉通岩石圈减薄的认识主要是基于对中国东部地区为主的金伯利岩携带的地幔橄榄岩捕虏体和橄榄石捕虏晶的研究提出的(郑建平, 1999; Xu, 2001; Menzies *et al.*, 1993; 池际尚和路凤香, 1996; Griffin *et al.*, 1998; Fan *et al.*, 2000; Gao *et al.*, 2002),最新的研究表明东西部岩石圈地幔减薄存在时空不均一性(Xu, 2007; 徐义刚, 2006b),但是对于西部岩石圈减薄的时空范围和造成这种岩石圈减薄的机制尚不清楚,有待进一步讨论。

基于以上问题,本文以重力梯度带附近的繁峙苏孟庄碱

性玄武岩和应县亚碱性玄武岩为研究对象,采用岩相学、元素及同位素地球化学等方法研究岩浆源区特征及岩浆演化过程。此外,我们还通过研究区新生代玄武岩与重力梯度带附近其他地区新生代玄武岩的对比,探讨重力梯度带附近玄武岩深部成因与地幔源区特征的异同性,并对重力梯度带附近地区新生代玄武岩的形成机制给出一个较为合理的解释。

## 1 地质背景

华北克拉通是世界上最古老的陆核之一(3.8 ~ 2.5Ga; Jahn *et al.*, 1987; Liu *et al.*, 1992),也是中国东部最为重要的地质构造单元。南以秦岭-大别-苏鲁造山带为界(Li *et al.*, 1993; Bai *et al.*, 2007; Meng and Zhang, 2000; Zhao and Zheng, 2009; Zheng *et al.*, 2013),北临中亚造山带(Windley *et al.*, 2007),西接青藏高原东北部,东连太平洋板块(Zheng *et al.*, 2013)。华北克拉通的东部地块和西部地块在 ~1.85Ga 时碰撞拼合,克拉通化,形成了一条南北贯穿克拉通的古元古代造山带——大兴安岭-太行山重力梯度带(Zhao *et al.*, 1999, 2001)。该带东、西两侧在地貌、地壳厚度、岩石圈厚度、地表热流值均存在明显的差异:东部地块的岩石圈较薄(<80km),地温梯度高,地表热流值高;西部岩石圈厚度大(100 ~ 150km),地温梯度低,地表热流值低(陈国英等, 1991; Niu, 2005; 徐义刚, 2006a)。在这一造山带的东缘发育着太行山断裂带。晚中生代以来大规模的伸展作用形成了华北克拉通内部广泛分布的北北东向裂谷系统:华北裂谷系、银川-河套和山西-陕西裂谷系(Ye *et al.*, 1987; Ren *et al.*, 2002; 图 1)。

前人根据对金伯利岩携带的地幔橄榄岩捕虏体和橄榄石捕虏晶的岩石学和矿物化学成分以及 Re-Os 同位素的研究指出,华北克拉通曾存在巨厚的太古代岩石圈地幔(>200km; 邓晋福, 1988; Menzies *et al.*, 1993; 池际尚和路凤香, 1996; Griffin *et al.*, 1998; Fan *et al.*, 2000; Gao *et al.*, 2002),在中生代时期发生了重要的岩石圈减薄事件,且重力梯度带东西两侧岩石圈的减薄存在时空上不均一性,导致了重力梯度带两侧岩石圈厚度的较大差异(Xu, 2007; 徐义刚, 2006a; Guo *et al.*, 2014),东部岩石圈在中生代经历了减薄(吴福元等, 2003),新生代以来逐渐增厚,而西部岩石圈主要在新生代发生减薄(徐义刚, 2006a)。

繁峙玄武岩位于华北克拉通大兴安岭-太行山重力梯度

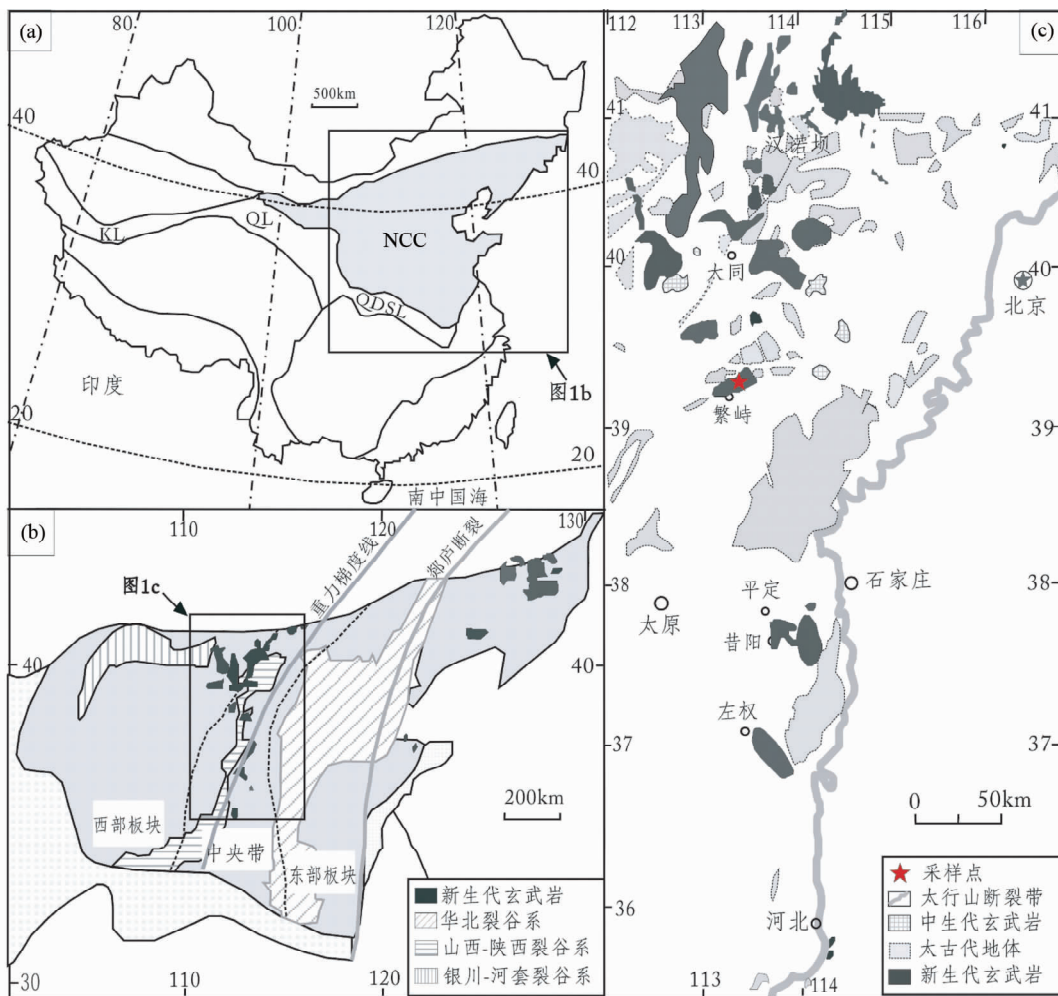


图 1 繁峙地区地质图

(a) 华北克拉通位置图; (b) 华北克拉通的三分 (东部地块、西部地块和中央带) 以及新生代裂谷系分布图 (据 Zhao *et al.*, 2001 修改); (c) 太行山新生代玄武岩、中生代侵入岩和太古代地体分布图 (据吴雅颂和王兴武, 1978<sup>①</sup>修改)

Fig. 1 Geological map in the Fanshi region

(a) location of the North China Craton; (b) three subdivisions of the craton and the distribution of Cenozoic rift systems (modified after Zhao *et al.*, 2001); (c) distribution of the Cenozoic basalts, Mesozoic intrusive rocks and Archean terrains in the Taihang mountains

带附近, 构造上位于恒山山脉东段南麓、山西断隆-五台隆起北东部。繁峙地区发育有滹沱河新裂陷, 在约 30 亿年的地质历史中, 经历了复杂的构造、沉积、岩浆、变质等地质作用, 尤其是新生代以来, 可能是太平洋板块的俯冲和印度-欧亚陆-陆碰撞的共同结果, 该区地质构造运动活跃, 繁峙玄武岩火山作用可能是这一大规模区域构造活动的局部响应。繁峙玄武岩之下的古老基底主要由角闪岩相到麻粒岩相的太古代片麻岩和绿岩以及碎屑岩夹层构成, 之上覆盖的是静乐红土层, 以及其他上新统、更新统的沉积物。玄武岩出露面积约 550 km<sup>2</sup>, 厚约 800 m, 最大倾角 < 15°, 本文样品采集于繁峙县城城北的苏孟庄岩体和大石线 S205 上靠近应县的川草坪岩体 (即后文中的应县玄武岩), 苏孟庄玄武岩主要属于碱

性系列, 底部携带有大量的地幔橄榄岩包体, 应县玄武岩属于亚碱性系列, 不含包体。全岩 K-Ar 年龄为 26.3 ~ 24.3 Ma (Tang *et al.*, 2006), 属于新生代渐新世玄武岩 (图 1)。

## 2 样品的采集和分析

苏孟庄碱性玄武岩主要分为重要的两层: 顶层样品主要为灰黑色气孔状玄武岩, 有些气孔中充填有方解石或其它碳酸盐矿物, 呈杏仁状构造; 底层样品为黑色致密块状玄武岩, 其中含有丰富地幔橄榄岩包体, 但与汉诺坝玄武岩不同的是, 包体主要为尖晶石二辉橄榄岩相, 没有发现辉石岩和麻粒岩。包体中的橄榄石蚀变较严重, 一般为中粒至粗粒结构

① 吴雅颂, 王兴武. 1978. 山西的近期玄武岩. 山西省地质局区域地质调查队, 1-136

表1 繁峙新生代玄武岩主量元素(wt%)

Table 1 Major elements data (wt%) of basalts from Fanshi

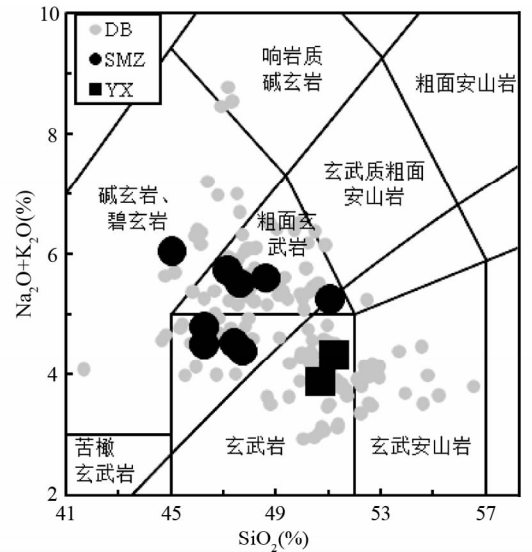
样品号	06	11	17	20	24	28	30	33	36	01	04
岩体	苏孟庄(SMZ11-)					应县(YX11-)					
SiO <sub>2</sub>	45.96	45.07	45.44	43.39	46.65	47.57	46.58	44.22	50.02	49.34	50.54
TiO <sub>2</sub>	2.25	2.46	2.38	2.39	2.54	2.26	2.34	2.39	2.26	1.92	2.07
Al <sub>2</sub> O <sub>3</sub>	15.51	13.88	14.24	12.72	12.93	13.59	13.68	14.33	13.41	14.00	13.84
Fe <sub>2</sub> O <sub>3</sub> <sup>T</sup>	11.70	12.70	11.92	11.80	12.80	11.95	12.22	12.85	11.02	11.38	12.04
MnO	0.17	0.17	0.17	0.16	0.16	0.16	0.17	0.17	0.15	0.15	0.16
MgO	7.74	9.00	9.00	8.03	9.53	8.41	8.74	9.47	7.88	8.27	7.60
CaO	8.50	8.66	9.91	7.49	8.13	7.61	7.88	8.10	7.29	8.06	7.60
Na <sub>2</sub> O	3.12	3.46	3.37	4.30	3.47	3.78	3.54	3.92	3.27	2.57	2.82
K <sub>2</sub> O	1.26	1.20	1.03	0.95	0.80	1.71	1.85	2.00	1.86	1.21	1.44
P <sub>2</sub> O <sub>5</sub>	0.65	0.76	0.72	0.75	0.65	0.74	0.72	0.78	0.73	0.36	0.49
LOI	2.57	2.10	1.27	7.48	1.77	1.64	1.72	1.24	1.53	2.10	0.80
Total	96.84	97.35	98.18	91.98	97.68	97.79	97.72	98.23	97.88	97.26	98.58
Mg <sup>#</sup>	56.7	58.4	60.0	57.4	59.6	58.2	58.6	59.3	58.6	59.0	55.6
Na <sub>2</sub> O + K <sub>2</sub> O	4.37	4.66	4.40	5.25	4.27	5.49	5.40	5.92	5.12	3.78	4.25
Na <sub>2</sub> O/K <sub>2</sub> O	2.48	2.89	3.26	4.54	4.34	2.21	1.91	1.96	1.76	2.12	1.96

注: Mg<sup>#</sup> = 100 × molar Mg / (Mg + Fe<sub>tot</sub><sup>2+</sup>)

不等,呈浅黄绿色至深黄绿色,部分矿物颗粒因为氧化蚀变颜色深暗。玄武岩镜下主要为斑状结构,斑晶以橄榄石为主,橄榄石斑晶粒径可达3mm,呈自形-半自形,短柱状或不规则颗粒状,裂理发育,正高突起,少量发生伊丁石化,除橄榄石斑晶以外,还存在少量磁铁矿斑晶和较多的斜长石微晶。包体以尖晶石相二辉橄榄岩为主,橄榄石占70%,单斜辉石14%,斜方辉石12%,尖晶石3%,磁铁矿1%,与中国东部的地幔捕虏体相似。应县亚碱性玄武岩主要呈灰黑色致密块状结构,镜下斑晶主要为单斜辉石和橄榄石,单斜辉石呈聚晶出现,斜长石穿插其中,单斜辉石聚晶含量约占15%~20%,自形-半自形,干涉色可达II级蓝,基质为斜长石微晶、磁铁矿以及火山玻璃等。

挑选较新鲜且具代表性的样品,切成薄片,用石英砂磨盘磨去锯痕及风化面,用碎样器粗碎至5mm,剔除样品中的杏仁体和斑晶,用去离子水在超声波中清洗两次,放烘箱中烘干样品,最后用玛瑙研磨仪磨至200目粉末。全岩主微量元素的分析在中国地质大学(北京)地质过程与矿产资源国家重点实验室完成,主量元素采用碱熔法,用电感耦合等离子发射光谱仪(ICP-OES)测试,测试精度1%~3%,分析结果见表1;微量元素采用混合酸溶样法,样品测定选用Agilent 7500a型四极杆电感耦合等离子体质谱仪(ICP-MS)进行测定,分析精度依所测元素的浓度高低变化于5%~15%之间,分析结果见表2。主微量元素详细的分析流程见Song *et al.* (2010)。

Sr-Nd-Pb-Hf 同位素样品分离在中国科学院地质与地球物理研究所同位素超净实验室完成,详细的分离流程见Chu *et al.* (2009)。Sr同位素比值测试分析在天津地质矿床研究所同位素实验室用 Triton 热电质谱仪(TIMS)上完成(见李潮峰等,2011),Nd和Pb同位素在中国地质大学(武汉)地质

图2 玄武岩 SiO<sub>2</sub>-(Na<sub>2</sub>O + K<sub>2</sub>O)图解

DB为前人重力梯度带附近的新生代玄武岩数据(Fan and Hopper, 1991; Tang *et al.*, 2006; 马金龙和徐义刚, 2004; Xu *et al.*, 2005; 张文慧等, 2005; Zhang *et al.*, 2012a, b; 朱昱升等, 2012); SMZ为采自苏孟庄的玄武岩样品, YX为采自靠近应县的川草坪岩体的样品,图3-图8同

Fig. 2 SiO<sub>2</sub> vs. Na<sub>2</sub>O + K<sub>2</sub>O diagram showing our studied samples from Sumengzhuang (SMZ) and Chuancaoping near Yingxian (YX)

For comparison, the literature data (DB) of the Cenozoic basalts near Taihang mountains are also plotted (data sources: Fan and Hopper, 1991; Tang *et al.*, 2006; Ma and Xu, 2004; Xu *et al.*, 2005; Zhang *et al.*, 2005, 2012a, b; Zhu *et al.*, 2012). SMZ are basalts we collected from Sumengzhuang; and YX are our basalts from Chuancaoping near Yingxian. Fig. 3 to Fig. 8 are same

表 2 繁峙新生代玄武岩微量元素 ( $\times 10^{-6}$ )Table 2 Trace elements data ( $\times 10^{-6}$ ) of basalts from Fanshi

样品号	06	11	17	20	24	28	30	33	36	01	04
岩体	苏孟庄(SMZ11-)									应县(YX11-)	
Li	5.40	6.25	5.20	6.35	5.52	5.38	5.95	6.95	5.37	4.89	5.06
P	2718	3214	3052	3466	2918	3056	3042	3182	3124	1516	2180
K	10098	10248	8812	8718	7012	14126	15408	16460	15784	10232	12208
Sc	17.1	17.1	23.2	15.3	17.3	14.1	15.4	15.8	14.0	21.4	18.5
Ti	14144	16332	15536	16882	16926	14428	15218	15132	15558	12632	14226
V	184	178	223	176	194	152	166	160	159	186	178
Cr	98.5	156	206	156	178	148	165	175	159	210	183
Mn	1085	1133	1172	1162	1164	1100	1115	1112	1065	1052	1104
Co	38.1	45.5	44.1	44.6	50.0	39.9	42.5	44.0	41.0	40.4	44.1
Ni	78.6	150	122	133	179	126	135	156	131	116	161
Cu	46.6	46.4	45.1	42.9	45.5	39.1	39.2	43.2	37.5	45.2	51.4
Zn	96.1	106	101	111	107	125	113	120	107	100	98.1
Ga	19.2	20.2	18.5	22.1	21.3	21.0	21.8	21.5	20.7	18.2	18.9
Rb	16.5	21.8	21.2	8.3	18.1	14.2	15.6	15.4	14.8	11.4	10.9
Sr	804	800	962	927	825	902	976	911	1000	464	613
Y	22.5	20.5	22.6	20.6	18.8	19.0	19.5	19.6	16.9	18.9	18.2
Zr	263	274	261	308	258	322	320	316	340	178	223
Nb	53.3	64.3	56.1	71.2	58.1	71.2	69.4	69.0	70.1	31.8	38.9
Cs	0.87	0.34	0.62	0.34	0.37	0.40	0.42	0.42	0.41	0.11	0.15
Ba	5368	409	868	500	357	520	512	521	543	387	424
La	32.6	33.7	34.7	38.4	28.6	36.6	36.1	35.7	34.5	17.8	22.6
Ce	66.4	66.8	71.1	77.1	58.0	74.3	73.2	73.0	71.8	38.1	46.2
Pr	8.72	8.73	9.27	9.96	7.68	9.64	9.65	9.54	8.68	5.22	5.80
Nd	32.8	33.4	35.1	38.1	30.0	36.4	36.8	36.4	36.1	20.7	24.7
Sm	6.57	7.04	7.01	7.85	6.48	7.43	7.58	7.42	7.45	4.66	5.52
Eu	2.55	2.27	2.22	2.53	2.12	2.35	2.40	2.36	2.40	1.58	1.84
Gd	6.10	6.37	6.24	6.90	5.91	6.43	6.59	6.47	6.52	4.59	5.30
Tb	0.89	0.93	0.92	0.99	0.87	0.91	0.94	0.93	0.86	0.73	0.75
Dy	4.41	4.43	4.51	4.55	4.10	4.21	4.35	4.29	4.28	3.73	4.14
Ho	0.90	0.84	0.91	0.83	0.77	0.77	0.79	0.79	0.71	0.76	0.76
Er	2.17	1.89	2.16	1.82	1.70	1.71	1.77	1.78	1.74	1.85	1.99
Tm	0.32	0.26	0.32	0.25	0.24	0.23	0.24	0.25	0.22	0.27	0.26
Yb	1.78	1.40	1.76	1.28	1.24	1.22	1.28	1.30	1.25	1.52	1.61
Lu	0.26	0.20	0.26	0.18	0.18	0.17	0.18	0.18	0.18	0.22	0.23
Hf	6.05	6.52	5.92	7.08	6.33	7.30	7.34	7.26	7.83	4.30	5.43
Ta	3.35	4.12	3.43	4.48	3.78	4.55	4.54	4.46	4.40	2.12	2.42
Pb	3.07	2.84	3.06	3.06	2.68	2.93	2.73	3.04	2.50	2.01	2.12
Th	2.85	2.90	3.00	3.22	2.51	3.25	3.20	3.14	2.86	1.41	1.66
U	0.80	0.97	0.85	1.08	0.86	1.10	1.09	1.07	1.04	0.45	0.55
La/Nb	0.61	0.52	0.62	0.54	0.49	0.51	0.52	0.52	0.49	0.56	0.58
Ba/Nb	101	6.36	15.5	7.02	6.14	7.30	7.38	7.54	7.74	12.2	10.9
Nb/U	66.6	66.4	66.1	65.8	67.6	65.0	63.8	64.7	67.7	71.5	70.1
Ce/Pb	21.6	23.5	23.2	25.2	21.7	25.4	26.8	24.1	28.7	18.9	21.8
La/Ce	0.49	0.50	0.49	0.50	0.49	0.49	0.49	0.49	0.48	0.47	0.49
Nb/La	1.63	1.91	1.62	1.86	2.03	1.94	1.92	1.93	2.04	1.79	1.72
Th/Ta	0.85	0.71	0.87	0.72	0.66	0.71	0.71	0.71	0.65	0.67	0.68

过程与矿产资源国家重点实验室用多接收等离子体质谱仪 (MC-ICP-MS) 测定, Hf 同位素在中国科学院地质与地球物理研究所用 MC-ICP-MS 分析, Sr-Nd-Hf 同位素的分馏分别采用  $^{86}\text{Sr}/^{88}\text{Sr} = 0.1194$ ,  $^{146}\text{Nd}/^{144}\text{Nd} = 0.7219$  和  $^{179}\text{Hf}/^{177}\text{Hf} = 0.7325$  进行指数法校正, 标样分析结果分别为: NBS-987 Sr 为  $^{87}\text{Sr}/^{86}\text{Sr} = 0.710245 \pm 16$ , JNdi-1 Nd 为  $^{143}\text{Nd}/^{144}\text{Nd} = 0.512118 \pm 12$ , Alfa Hf  $^{176}\text{Hf}/^{177}\text{Hf}$  为  $0.282179 \pm 4$ , NBS-981 Pb 标样得到  $^{206}\text{Pb}/^{204}\text{Pb} = 16.915 \pm 10$ ,  $^{207}\text{Pb}/^{204}\text{Pb} = 15.465 \pm$

$9$ ,  $^{208}\text{Pb}/^{204}\text{Pb} = 36.617 \pm 11$ 。样品分析结果见表 3。

## 3 分析结果

### 3.1 主量元素

在 TAS 图解 (图 2) 中, 苏孟庄采集的玄武岩基本落在碱性系列中, 顶层样品主要属于玄武岩, 底层样品主要属于粗面玄武岩和碱玄岩/碧玄岩; 应县采集的样品均落在亚碱性

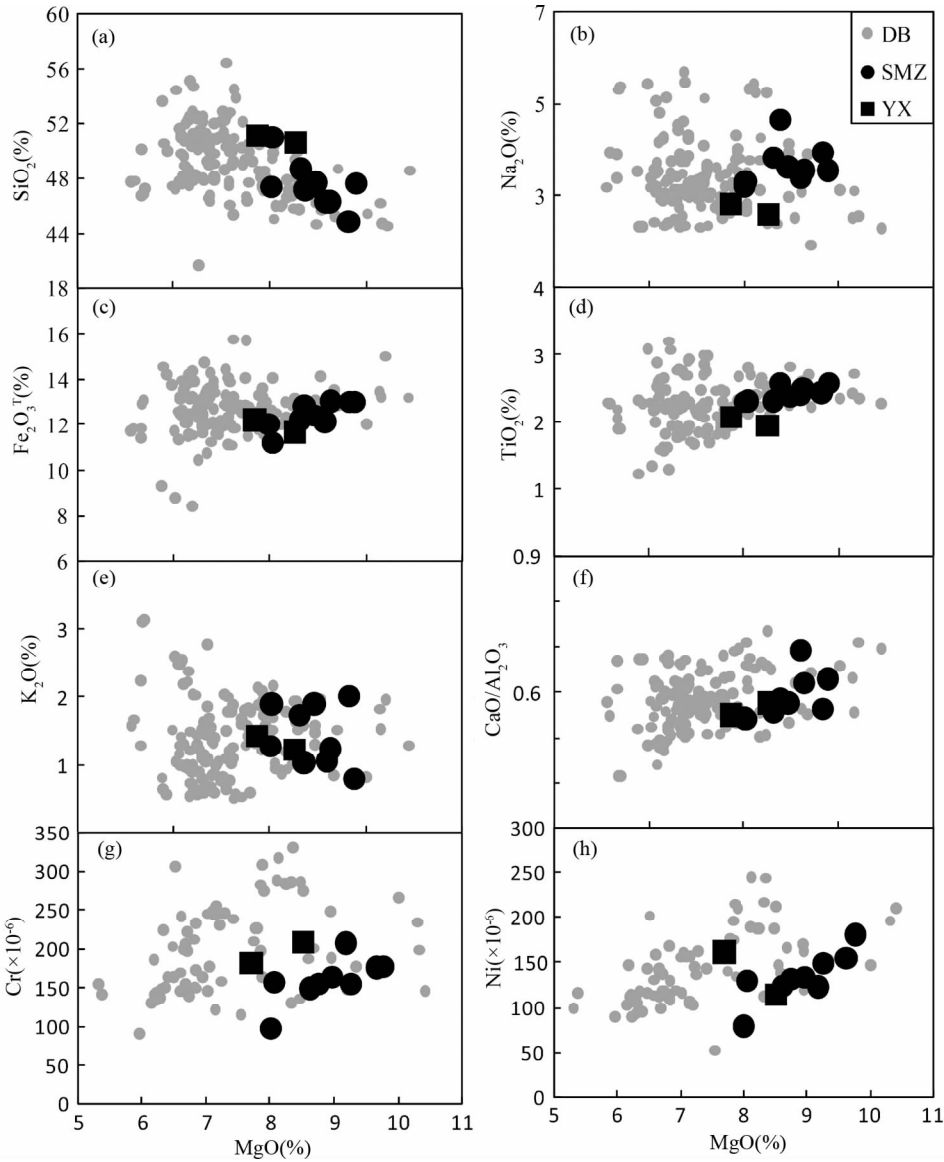


图3 繁峙新生代玄武岩主要元素氧化物及微量元素 Cr、Ni 对 MgO 的协和图

Fig.3 Various oxides and Cr, Ni plotted against MgO for Cenozoic basalts in Fanshi with literature data plotted for comparison

表3 繁峙新生代玄武岩全岩 Sr-Nd-Pb-Hf 同位素组成

Table 3 Sr-Nd-Pb-Hf isotopic compositions of basalts from Fanshi

岩体	样品号	$\frac{87}{86}\text{Rb}/\frac{86}{86}\text{Sr}$	$\frac{87}{86}\text{Sr}/\frac{86}{86}\text{Sr} (2\sigma)$	$\frac{147}{144}\text{Sm}/\frac{144}{144}\text{Nd}$	$\frac{143}{144}\text{Nd}/\frac{144}{144}\text{Nd} (2\sigma)$	$\epsilon_{\text{Nd}}(t)$	$\frac{208}{204}\text{Pb}/\frac{204}{204}\text{Pb} (2s)$	$\frac{207}{204}\text{Pb}/\frac{204}{204}\text{Pb} (2s)$	$\frac{206}{204}\text{Pb}/\frac{204}{204}\text{Pb} (2s)$	$\frac{176}{177}\text{Lu}/\frac{177}{177}\text{Hf}$	$\frac{176}{177}\text{Hf}/\frac{177}{177}\text{Hf} (2\sigma)$	$\epsilon_{\text{Hf}}(t)$
苏孟庄	SMZ11-17	0.0639	0.704870 ± 3	0.1268	0.512689 ± 6	1.23	37.6 ± 10	15.4 ± 4	17.6 ± 4	0.0060	0.282948 ± 12	6.68
	SMZ11-24	0.0638	0.703848 ± 3	0.1373	0.513057 ± 4	8.36	37.8 ± 11	15.4 ± 4	17.9 ± 5	0.0039	0.283001 ± 12	8.60
	SMZ11-33	0.0491	0.703979 ± 4	0.1295	0.512804 ± 3	3.45	37.9 ± 12	15.4 ± 5	17.9 ± 4	0.0035	0.282998 ± 10	8.51
	SMZ11-36	0.0431	0.703937 ± 2	0.1310	0.512904 ± 2	5.40	37.9 ± 8	15.4 ± 3	17.9 ± 3	0.0031	0.282996 ± 10	8.42
应县	YX11-01	0.0712	0.704732 ± 3	0.1430	0.512932 ± 5	5.91	37.5 ± 10	15.3 ± 4	17.2 ± 4	0.0071	0.282873 ± 17	4.00
	YX11-04	0.0519	0.704398 ± 3	0.1417	0.512617 ± 3	-0.23	37.5 ± 6	15.4 ± 2	17.3 ± 2	0.0059	0.282879 ± 17	4.23

注:  $\epsilon_{\text{Nd}}(t) = \{ [ ( ^{143}\text{Nd}/^{144}\text{Nd} )_s - ( ^{147}\text{Sm}/^{144}\text{Nd} )_s \times ( e^{\lambda t} - 1 ) ] / [ ( ^{143}\text{Nd}/^{144}\text{Nd} )_{\text{CHUR}} - ( ^{147}\text{Sm}/^{144}\text{Nd} )_{\text{CHUR}} \times ( e^{\lambda t} - 1 ) ] - 1 \} \times 10^4$ , 其中,  $( ^{143}\text{Nd}/^{144}\text{Nd} )_{\text{CHUR}} = 0.512638$ ,  $( ^{147}\text{Sm}/^{144}\text{Nd} )_{\text{CHUR}} = 0.1967$ ,  $\lambda$  为  $6.54 \times 10^{-12} \text{ a}^{-1}$ ;  $\epsilon_{\text{Hf}}(t) = \{ [ ( ^{176}\text{Hf}/^{177}\text{Hf} )_s - ( ^{176}\text{Lu}/^{177}\text{Hf} )_s \times ( e^{\lambda t} - 1 ) ] / [ ( ^{176}\text{Hf}/^{177}\text{Hf} )_{\text{CHUR}} - ( ^{176}\text{Lu}/^{177}\text{Hf} )_{\text{CHUR}} \times ( e^{\lambda t} - 1 ) ] - 1 \} \times 10^4$ , 其中,  $( ^{176}\text{Hf}/^{177}\text{Hf} )_{\text{CHUR}} = 0.282772$ ,  $( ^{176}\text{Lu}/^{177}\text{Hf} )_{\text{CHUR}} = 0.0332$ ,  $\lambda$  为  $1.867 \times 10^{-11} \text{ a}^{-1}$ ; 繁峙玄武岩用  $t = 25.3 \text{ Ma}$  来校正

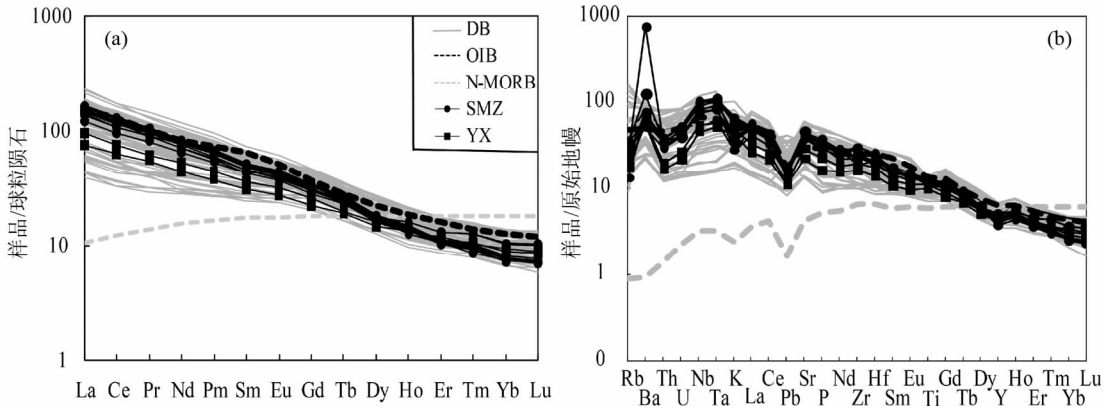


图4 繁峙玄武岩稀土元素球粒陨石标准化配分图(a)和不相容元素原始地幔标准化蛛网图(b)

数据来源:原始地幔、球粒陨石、N-MORB、OIB(Sun and McDonough, 1989),DB为前人重力梯度带附近的新生代玄武岩数据(Tang *et al.*, 2006; 马金龙和徐义刚, 2004; 张文慧等, 2005; 朱昱升等, 2012)

Fig.4 Chondrite-normalized REE patterns (a) and primitive mantle normalized incompatible element diagrams (b) for basalts in Fanshi

Normalization values PM, CHUR, N-MORB and OIB after Sun and McDonough, 1989; DB after Tang *et al.*, 2006; Ma and Xu, 2004; Zhang *et al.*, 2005; Zhu *et al.*, 2012

系列中。因此本文认为苏孟庄玄武岩可能是多阶段喷发的结果,至少可分为重要的两层,顶层以碱性玄武岩为主,底层以粗面玄武岩为主,苏孟庄最底层样品几乎落在碱性系列和亚碱性的分界线上,可能暗示着一个由碱性到亚碱性的过渡转变。

繁峙玄武岩主量元素分析结果见表1,其 $\text{SiO}_2$ 含量介于43.39%~50.54%, $\text{TiO}_2$ 为1.92%~2.54%, $\text{K}_2\text{O} + \text{Na}_2\text{O}$ 值为3.78%~5.92%, $\text{Na}_2\text{O}/\text{K}_2\text{O}$ 比值为1.76~4.54,全铁 $\text{Fe}_2\text{O}_3^{\text{T}}$ 为11.02%~12.85%, $\text{Mg}^{\#}$ 为55.6~60.0。从主量元素氧化物及微量元素对 $\text{MgO}$ 的协和图中可以看出, $\text{SiO}_2$ 与 $\text{MgO}$ 呈简单的负相关关系, $\text{TiO}_2$ 、 $\text{Fe}_2\text{O}_3^{\text{T}}$ 和 $\text{CaO}/\text{Al}_2\text{O}_3$ 与 $\text{MgO}$ 呈简单的正相关关系, $\text{Na}_2\text{O}$ 、 $\text{K}_2\text{O}$ 随 $\text{MgO}$ 的降低变化不明显,微量元素Cr、Ni与 $\text{MgO}$ 大致呈正相关关系(图3)。此外,苏孟庄碱性玄武岩和应县亚碱性玄武岩在成分上存在差异,应县玄武岩的 $\text{SiO}_2$ 含量相较苏孟庄偏高, $\text{TiO}_2$ 、 $\text{Na}_2\text{O}$ 、 $\text{P}_2\text{O}_5$ 较苏孟庄玄武岩低,这可能与岩浆源区和熔融条件有关。

### 3.2 微量元素地球化学

繁峙玄武岩的稀土元素(REE)总量总体偏高,苏孟庄玄武岩为 $149.7 \times 10^{-6} \sim 192.8 \times 10^{-6}$ ,应县玄武岩为 $103.1 \times 10^{-6} \sim 123.0 \times 10^{-6}$ ,应县玄武岩相对苏孟庄明显偏低。稀土元素球粒陨石标准化配分图(图4a)显示该地区玄武岩都具有LREEs富集,HREEs亏损的特点,轻重稀土分馏明显,呈右倾模式,只是苏孟庄和应县的分馏程度不同,苏孟庄玄武岩 $(\text{La}/\text{Yb})_{\text{N}}$ 为13.3~21.6, $(\text{La}/\text{Sm})_{\text{N}}$ 为2.78~3.20, $(\text{Gd}/\text{Yb})_{\text{N}}$ 为2.79~4.30,而应县两样品的 $(\text{La}/\text{Yb})_{\text{N}} < 10$ , $(\text{La}/\text{Sm})_{\text{N}} < 2.6$ , $(\text{Gd}/\text{Yb})_{\text{N}} < 2.7$ ,苏孟庄玄武岩的分馏程度明显高于应县玄武岩。Sr、Eu元素无亏损,Eu甚至轻微富

集, $\text{Eu}/\text{Eu}^*$  ( $\text{Eu}/\text{Eu}^* = (\text{Sm} + \text{Gd})/2\text{Eu}$ )介于1.00~1.21之间。

原始地幔(PM)标准化微量元素蛛网图中(图4b),繁峙玄武岩显示了与洋岛玄武岩(OIB)类似的特征,随着元素不相容性的升高而富集。采样点的玄武岩均富集Rb、Ba、Th、U、Sr等大离子亲石元素(LILE),不亏损Nb、Ta、Zr、Hf等高场强元素(HFSE),且Nb和Ta相对富集。繁峙玄武岩的Ce/Pb、Nb/U比值较高,La/Nb、Ba/Nb比值较低(图5),同样与OIB相似。以上微量元素特征暗示繁峙玄武岩与OIB具有相似的源区。

### 3.3 Sr-Nd-Pb-Hf 同位素特征

所测6个样品的Sr同位素比值较低( $^{87}\text{Sr}/^{86}\text{Sr} = 0.703848 \sim 0.704870$ ),Nd、Hf同位素比值较高,分别为 $^{143}\text{Nd}/^{144}\text{Nd} = 0.512617 \sim 0.513057$ 和 $^{176}\text{Hf}/^{177}\text{Hf} = 0.282873 \sim 0.283001$ , $\varepsilon_{\text{Nd}}(t) = -0.23 \sim 8.36$ , $\varepsilon_{\text{Hf}}(t) = 4.00 \sim 8.60$ (表3)。 $^{87}\text{Sr}/^{86}\text{Sr}$ - $^{143}\text{Nd}/^{144}\text{Nd}$ 图(图6a)可以看出苏孟庄碱性玄武岩和应县亚碱性玄武岩投点均位于洋岛玄武岩(OIB)区域,接近全硅酸盐地球值(BSE),投点总体呈负相关关系。 $\varepsilon_{\text{Nd}}(t)$ - $\varepsilon_{\text{Hf}}(t)$ 图解(图6b)中研究区样品基本投在OIB区域,全球阵列参考线附近, $\varepsilon_{\text{Nd}}(t)$ 与 $\varepsilon_{\text{Hf}}(t)$ 呈近似正相关关系。

6个样品的 $^{206}\text{Pb}/^{204}\text{Pb}$ 比值在17.2~17.9之间, $^{207}\text{Pb}/^{204}\text{Pb}$ 和 $^{208}\text{Pb}/^{204}\text{Pb}$ 比值范围分别为15.3~15.4和37.5~37.9,且苏孟庄碱性玄武岩Pb同位素比值整体高于应县亚碱性玄武岩。从 $^{206}\text{Pb}/^{204}\text{Pb}$ - $^{208}\text{Pb}/^{204}\text{Pb}$ 图可见(图7a),碱性玄武岩基本落在印度洋MORB范围内,平行于北半球参照线(NHRL),与汉诺坝玄武岩类似,亚碱性玄武岩则靠近五大连池岩体。在 $^{206}\text{Pb}/^{204}\text{Pb}$ - $^{207}\text{Pb}/^{204}\text{Pb}$ 图中(图7b),

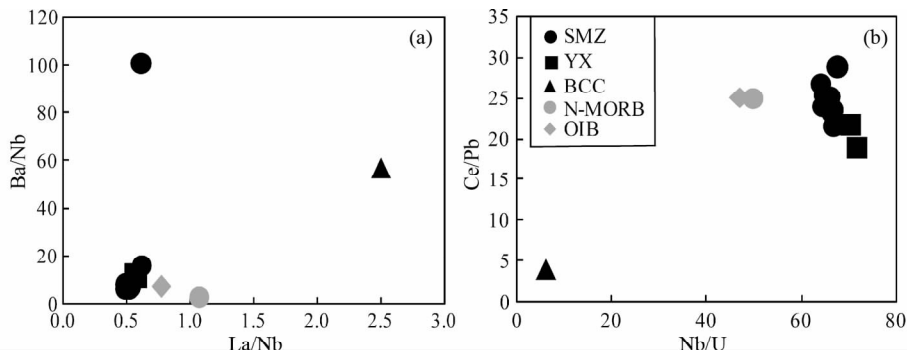


图5 繁峙玄武岩的 La/Nb-Ba/Nb (a) 和 Nb/U-Ce/Pb (b) 图解

数据来源: N-MORB、OIB (Sun and McDonough, 1989); BCC (Rudnick and Gao, 2003)

Fig. 5 La/Nb vs. Ba/Nb (a) and Nb/U vs. Ce/Pb (b) plots for the Cenozoic basalts

Data sources: N-MORB, OIB (Sun and McDonough, 1989), BCC (Rudnick and Gao, 2003)

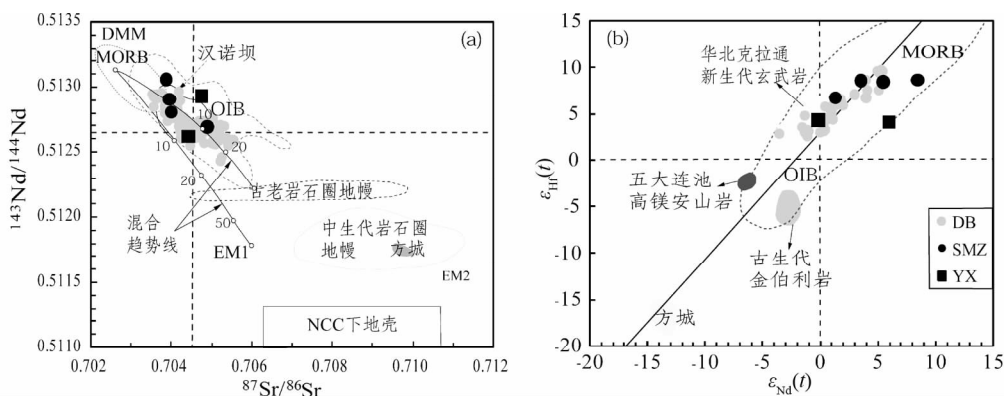


图6 繁峙新生代玄武岩的  $^{87}\text{Sr}/^{86}\text{Sr}$ - $^{143}\text{Nd}/^{144}\text{Nd}$  图解 (a) 和  $\epsilon_{\text{Nd}}(t)$ - $\epsilon_{\text{Hf}}(t)$  图解 (b)

图6a中数据来源: 汉诺坝玄武岩 (Song *et al.*, 1990; Zhi *et al.*, 1990; Basu *et al.*, 1991; 解广轰和王俊文, 1992); 白垩纪方城玄武岩、中生代岩石圈地幔和华北克拉通 (NCC) 岩石圈地幔 (Zhang *et al.*, 2002); NCC 下地壳 (Jahn *et al.*, 1999); MORB, OIB, EMI 和 EM2 (Zindler and Hart, 1986); DB (Tang *et al.*, 2006; 马金龙和徐义刚, 2004; Xu *et al.*, 2005; 张文慧等, 2005; Zhang *et al.*, 2012a, b; 朱昱升等, 2012); 图6b 数据来源: 中生代金伯利岩和中生代方城玄武岩 (Zhang *et al.*, 2002); 五大连池高镁安山岩 (Zhang *et al.*, 2003); DB (Zhang *et al.*, 2012b; 朱昱升等, 2012); 全球阵列参考线 ( $\epsilon_{\text{Hf}} = 1.36\epsilon_{\text{Nd}} + 2.95$ , Vervoort and Blichert-Toft, 1999)

Fig. 6  $^{87}\text{Sr}/^{86}\text{Sr}$  vs.  $^{143}\text{Nd}/^{144}\text{Nd}$  (a) and  $\epsilon_{\text{Nd}}(t)$  vs.  $\epsilon_{\text{Hf}}(t)$  (b) diagrams for Fanshi Cenozoic basalts

Data sources in Fig. 6a: Hannuoba basalts (Song *et al.*, 1990; Zhi *et al.*, 1990; Basu *et al.*, 1991; Xie and Wang, 1992), Cretaceous Fangcheng basalts, Mesozoic lithospheric mantle and old lithospheric mantle beneath the NCC (Zhang *et al.*, 2002), lower crust of the NCC (Jahn *et al.*, 1999), MORB, OIB, EMI and EM2 (Zindler and Hart, 1986); DB (Tang *et al.*, 2006; Ma and Xu, 2004; Xu *et al.*, 2005; Zhang *et al.*, 2005, 2012a, b; Zhu *et al.*, 2012); Data source in Fig. 6b: Paleozoic kimberlite and Mesozoic basalts from Fangcheng (Zhang *et al.*, 2002), Wulanhada high-Mg andisite (Zhang *et al.*, 2003); DB (Zhang *et al.*, 2012b; Zhu *et al.*, 2012); Reference Terrestrial Array ( $\epsilon_{\text{Hf}} = 1.36\epsilon_{\text{Nd}} + 2.95$ ) is after Vervoort and Blichert-Toft (1999)

样品投点均落在 NHRL 附近。总体来说, 繁峙玄武岩在同位素组成上与重力梯度带附近的新生代玄武岩有着相似的特征 (Tang *et al.*, 2006; 马金龙和徐义刚, 2004; Xu *et al.*, 2005; 张文慧等, 2005; Zhang *et al.*, 2012a, b; 朱昱升等, 2012), 都具有类 OIB 的同位素组成。

## 4 讨论

### 4.1 地壳混染作用

大陆背景下的地幔派生岩浆在上升喷发过程中会通过

比大洋地区更厚的地壳, 难免会受到不同程度地壳混染作用, 因此所显现出来的地球化学特征要比大洋玄武岩更加复杂。但是观察表明地壳混染作用对繁峙玄武岩组成改变的影响可以忽略不计: (1) 在苏孟庄底层新生代玄武岩中发现有橄榄岩包体, 表明该地区的玄武岩是岩浆快速上升的结果, 在地壳中停留的时间较短, 因此在上升的过程中经历的地壳混染作用较小; (2) 从繁峙新生代玄武岩的地球化学特征来看, 繁峙新生代玄武岩具有与洋岛玄武岩以及汉诺坝玄武岩相似的地球化学特征, La/Nb-Ba/Nb 和 Nb/U-Ce/Pb 图 (图5) 显示繁峙玄武岩的不相容元素比值与 OIB、N-MORB



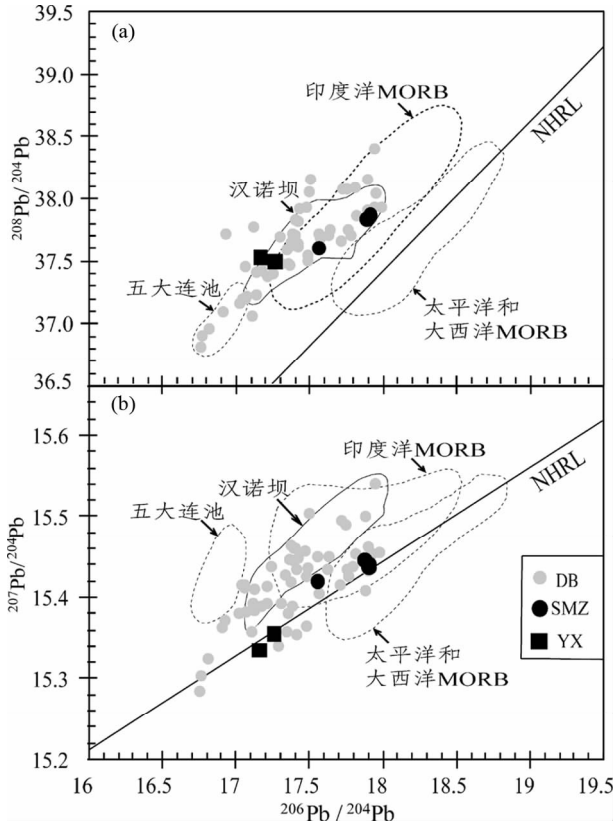


图7 繁峙新生代玄武岩的 $^{206}\text{Pb}/^{204}\text{Pb}$ - $^{208}\text{Pb}/^{204}\text{Pb}$  (a) 和 $^{206}\text{Pb}/^{204}\text{Pb}$ - $^{207}\text{Pb}/^{204}\text{Pb}$  (b) 图解

数据来源: 印度洋、太平洋和北大西洋 MORB (Barry and Kent, 1998; Zou *et al.*, 2000), NHRL (Hart, 1984), 五大连池玄武岩 (Zhang *et al.*, 1998; Zou *et al.*, 2003); DB 为前人重力梯度带附近的新生代玄武岩数据 (Tang *et al.*, 2006; 张文慧等, 2005; Zhang *et al.*, 2012b)

Fig. 7  $^{206}\text{Pb}/^{204}\text{Pb}$  vs.  $^{208}\text{Pb}/^{204}\text{Pb}$  (a) and  $^{206}\text{Pb}/^{204}\text{Pb}$  vs.  $^{207}\text{Pb}/^{204}\text{Pb}$  (b) diagrams for the Fanshi Cenozoic basalts  
Data sources: Indian MORB and Pacific and North Atlantic MORB (Barry and Kent, 1998; Zou *et al.*, 2000), NHRL (Hart, 1984), Wudalianchi basalts (Zhang *et al.*, 1998a; Zou *et al.*, 2003), DB (Tang *et al.*, 2006; Zhang *et al.*, 2005, 2012b)

相近, 离全大陆地壳 (BCC) 投点较远, 同样说明地壳混染不明显; (3) 如果玄武岩在上升的过程中受到的地壳混染程度较高, 将会赋予玄武岩较明显的“地壳特征”。平均全大陆地壳以 Nb、Ta、Ti 亏损为特征 (Sun and McDonough, 1989), 较低的 Nb、Ta 含量, 高的原始地幔标准化 Th/Nb 比值、低 Nb/La (<1) 比值、明显 Nb、Ta、Ti 负异常的微量元素配分模式, 是受到地壳混染的最鲜明的识别特征, 但是从繁峙玄武岩中并没有观察到这些特征, 繁峙玄武岩 Nb、Ta 富集、 $(\text{Th}/\text{Nb})_{\text{N}} = 0.34 \sim 0.45$ 、 $(\text{Nb}/\text{La})_{\text{N}} = 1.57 \sim 1.96$ , 微量元素蛛网图中 Nb、Ta、Ti 呈正异常, 看不到“地壳特征”, 因此可以排除地壳混染的重要性。

一般认为不含包体的玄武岩因上升速度较慢而在地壳中停留的时间较长, 将能更高程度地同化地壳物质。应县亚

碱性玄武岩及苏孟庄上层不含包体的碱性玄武岩的 Nb、Ta 含量相对较低, 可能暗示着地壳混染程度较苏孟庄底层玄武岩高。但是整个繁峙玄武岩的地球化学特征总体上都与地壳混染程度较小的 OIB 和汉诺坝玄武岩相似 (Song *et al.*, 1990; Zhi *et al.*, 1990; Basu *et al.*, 1991), 表明地壳混染作用对繁峙玄武岩的地球化学特征的改变可忽略不计。

#### 4.2 分离结晶作用

繁峙玄武岩的  $\text{Mg}^{\#}$  为 55.6 ~ 60.0, 表明岩浆在演化过程中必然经历了一定程度的分离结晶作用。显微镜下观察到, 苏孟庄玄武岩中含有橄榄石 (ol) 斑晶, 斜长石 (pl) 微晶, 应县玄武岩中含有橄榄石、单斜辉石 (cpx) 斑晶。在无水或少水条件下 (如俯冲带岩浆作用条件), 橄榄石和单斜辉石同时在液相线的结晶表明高压条件下的结晶分异作用, 与岩石圈地幔条件岩浆房的推测一致。斜长石微晶是地表或近地表喷发时骤然降温冷却的结果。

微量元素蛛网图中 (图 4b), Eu 和 Sr 没有明显的负异常, 说明斜长石的分离结晶作用不明显,  $\text{CaO}/\text{Al}_2\text{O}_3$  与  $\text{MgO}$  呈正相关关系, 只是斜率较小, 是单斜辉石分离结晶的结果。苏孟庄玄武岩的 Cr、Ni 随  $\text{MgO}$  的减小呈明显的下降趋势, 表明苏孟庄玄武岩在上升过程中经历了橄榄石和单斜辉石的分离结晶。应县玄武岩的  $\text{MgO}$  含量相对较低, Cr、Ni 随  $\text{MgO}$  变化的趋势不明显, 说明橄榄石和单斜辉石的分离结晶作用较苏孟庄玄武岩弱。这些演化趋势均与重力梯度带附近的玄武岩相似 (Fan and Hopper, 1991; Basu *et al.*, 1991; Tang *et al.*, 2006; 马金龙和徐义刚, 2004; Xu *et al.*, 2005; 张文慧等, 2005; Zhang *et al.*, 2012a, b; 朱昱升等, 2012), 因此, 该地区的岩浆演化过程中橄榄石和单斜辉石是常见的分离结晶矿物。

#### 4.3 岩浆源区

繁峙玄武岩的主微量组成、Ba/Nb、La/Nb 和 Ce/Pb 等比值以及 Sr-Nd-Pb-Hf 同位素组成均与 OIB 及汉诺坝玄武岩相似 (Song *et al.*, 1990; Zhi *et al.*, 1990; Basu *et al.*, 1991; 解广轰和王俊文, 1992), 表明研究区玄武岩的源区与 OIB 及汉诺坝玄武岩相似, 可能均起源于软流圈地幔。结合前人的研究发现, 汉诺坝、大同、集宁、阳原、鹤壁新生代玄武岩同样具有该特征 (Song *et al.*, 1990; Zhi *et al.*, 1990; Basu *et al.*, 1991; Tang *et al.*, 2006; 马金龙和徐义刚, 2004; Xu *et al.*, 2005; 张文慧等, 2005; Zhang *et al.*, 2012a, b; 朱昱升等, 2012), 推断重力梯度带附近的这些新生代玄武岩可能起源于同一软流圈地幔源区。

繁峙玄武岩的地幔源区物质比 OIB、原始地幔更富集不相容元素 (Sun and McDonough, 1989),  $(\text{La}/\text{Sm})_{\text{繁峙玄武岩源区}} > (\text{La}/\text{Sm})_{\text{OIB源区}} > (\text{La}/\text{Sm})_{\text{PM}}$ , 并且越不相容的元素越富集 (图 4b), OIB 的这种富集特征被认为是洋壳物质 (Hofmann and White, 1982)、陆源沉积物 (White and Duncan, 1996;

Weaver, 1991)或者大陆岩石圈物质(McKenzie and O'Nions, 1983, 1995)加入到了源区的结果。然而循环洋壳(如(La/Sm)<sub>PM</sub> < 1)太亏损,陆源沉积物地壳特征(富集Pb,亏损Nb、Ta、P和Ti)太明显,都不适合作为OIB的源区物质(Niu and O'Hara, 2003; Niu *et al.*, 2011),因此岩石圈底部和地震波低速带(LVZ)顶部交界处富集组分以及岩石圈中的富集岩脉对熔体的交代作用是造成OIB富集特征最有可能的原因(Lambert and Wyllie, 1970; Niu and O'Hara, 2003, 2007<sup>①</sup>; Pilet *et al.*, 2005; Niu *et al.*, 2011)。对于远离板块边界的大陆背景下的玄武质岩浆作用,可能也存在类似的地幔交代作用。中国东部之下的地震波层析成像图显示:在中国东部之下410~660km过渡带内存在冷的太平洋俯冲板块,其中的挥发分和富集不相容元素的熔体在浮力的作用下会聚集在LVZ顶部,还有一些甚至上升结晶出液相矿物加入橄榄岩围岩,形成“堆晶”岩脉。软流圈地幔在上涌的过程中会与这些富熔体层和岩脉发生交代作用,使喷发的岩浆相比之前更加富集(O'Reilly and Griffin, 1988; Niu, 2008; Niu *et al.*, 2012)。

Sr-Nd-Hf(图6)以及Pb同位素图解(图7)可以看出:繁峙玄武岩同位素呈现亏损的特征,但与MORB相比,其Sr同位素比值相比较, Nd、Hf同位素比值相比较低,主要分布在OIB范围内,同位素都呈较良好的线性关系,这与中国东部的其他地区的新生代碱性玄武岩相似(Zhou and Armstrong, 1982; Zhang *et al.*, 2009; Wang *et al.*, 2011b),表明至少有两个地幔端元参与了繁峙玄武岩的成岩作用,即亏损地幔和富集地幔组分。亏损地幔指的是软流圈地幔可能还包括新生的岩石圈地幔,但是后者在没有更高温、新热源的情况下不参与岩浆作用;富集地幔组分可能是EM1(Zhou and Armstrong, 1982; Zhi *et al.*, 1990)或者EM2(Zou *et al.*, 2000)。对太行山地区玄武岩中携带的地幔橄榄岩包裹体以及中生代辉长岩的研究表明:太行山地区之下的岩石圈厚度约80~100km(Ma, 1989),且之下的岩石圈地幔具有类EM1型富集地幔特征,可能是经富集、交代后的古老岩石圈的残余(Tatsumoto *et al.*, 1992; Gao *et al.*, 2002; Zhang *et al.*, 2004; 汤艳杰等, 2004; Tang *et al.*, 2006, 2012; Rudnick *et al.*, 2006; Wang *et al.*, 2006; Huang *et al.*, 2012),因此,我们推断参与繁峙玄武岩成岩作用的富集端元极有可能是繁峙地区之下的具有EM1型特征的古老岩石圈地幔。但是华北克拉通之下的古老岩石圈地幔经历了大程度熔体的抽离,很难熔融生成大量镁铁质岩浆,因此,古老克拉通岩石圈地幔不可能是大陆玄武岩的主要源区。我们根据Sr-Nd同位素二端元混合模拟(图6a)得出富集组分 < 10%。

因此,我们推断繁峙新生代玄武岩主要起源于软流圈地幔的部分熔融,但存在软流圈-岩石圈的相互作用:少量EM1型古老岩石圈地幔的加入解释了繁峙玄武岩同位素总体上亏损,但相比MORB富集的特征,吸收岩石圈底部的富熔体

层和同化岩石圈中早期形成的交代岩脉解释了不相容元素富集的特征。

#### 4.4 熔融程度与深度

玄武岩的硅饱和程度和熔融深度有关(Green and O'Hara, 1971; DePaolo and Daley, 2000),实验岩石学得出硅不饱和的碱性岩浆产生的压力要高于硅饱和的拉斑玄武岩浆(Green and O'Hara, 1971; Falloon *et al.*, 1988; Kushiro, 2001)。一般认为华北的碱性玄武岩的源区压力为25~30kbar(>80km),拉斑玄武岩的源区压力为15~20kbar(50~60km; Nohda *et al.*, 1991)。苏孟庄玄武岩皆为碱性玄武岩,应县玄武岩为亚碱性玄武岩,且苏孟庄玄武岩相比应县玄武岩的SiO<sub>2</sub>的含量较低, LREE丰度较高, LREE/HREE值较大,暗示着苏孟玄武岩的熔融深度较应县玄武岩大。这种熔融深度的差异可能来自于地幔源区的不均一性,也可能来自于岩石圈的厚度的差异(Niu *et al.*, 2011)。

繁峙新生代玄武岩明显富集轻稀土元素,轻重稀土分馏明显,(La/Yb)<sub>N</sub>为8.42~21.60,呈明显的右倾模式,且苏孟庄玄武岩相比应县玄武岩分馏程度更加明显,表明繁峙玄武岩都起源于以石榴子石二辉橄榄岩为主的较深的深度,且苏孟庄玄武岩的熔融深度较应县玄武岩大。因为对于石榴子石, Yb是相容元素,而La、Sm为不相容元素,石榴子石相橄榄岩部分熔融的程度越低,分异程度越明显;而在尖晶石相橄榄岩部分熔融作用中, La/Yb变化较小、Sm/Yb基本不变,因此La/Yb-Sm/Yb图常用于区分来自石榴子石相橄榄岩和尖晶石相橄榄岩的玄武岩(Niu *et al.*, 1996; Xu *et al.*, 2005)。从繁峙玄武岩的La/Yb-Sm/Yb图中(图8a)可以看出,苏孟庄玄武岩和应县玄武岩都落在石榴子石二辉橄榄岩熔融模拟曲线上,且苏孟庄玄武岩较应县玄武岩的熔融程度低,苏孟庄约为1%~3%,应县玄武岩约为3%~5%。

高度不相容元素的比值可用于示踪岩石形成的过程。地幔岩浆作用过程中Zr相对于Y更不相容,不相容元素Zr/Y比值受部分熔融程度的影响,但基本不受分离结晶作用的影响,熔融程度越低,Zr/Y比值越高(Nicholson and Latin, 1992)。Zr-Zr/Y图中(图8b),样品所投的点相关性良好,具有一定的斜率,这说明研究区玄武岩主要起源于地幔物质的部分熔融,样品间化学组分的差异可能来源于不同深度地幔物质的不同程度的部分熔融和源区物质的不均一性。苏孟庄玄武岩样品的Zr/Y比值整体比应县的高,说明苏孟庄玄武岩的熔融程度较应县低,与La/Yb-Sm/Yb图得出的模拟计算结果一致。

① Niu YL and O'Hara MJ. 2007. "Mantle plumes" are NOT from ancient oceanic crust. <http://www.mantleplumes.org/NotFromCrust.html>

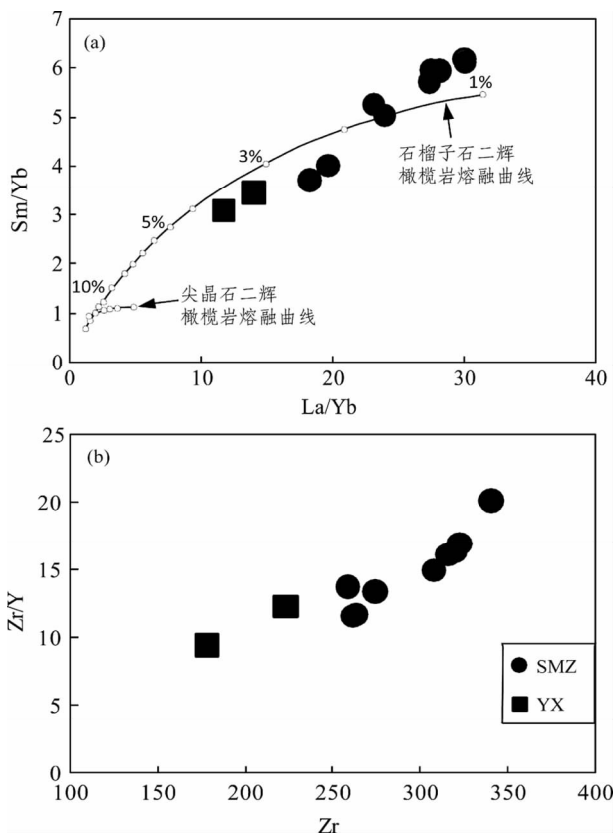


图8 La/Yb-Sm/Yb图(a)和Zr-Zr/Y图(b)用于判别岩浆的成岩过程

(a)图中:曲线旁数字代表熔融比例;源岩矿物组分和矿物熔融比例数据引自 Johnson *et al.* (1990),元素分配系数数据引自 McKenzie and O'Nions(1991)

Fig. 8 La/Yb vs. Sm/Yb (a) and Zr vs. Zr/Y (b) for Fanshi basalts

In Fig. 8a; the number near the curve are melting ratio; Source rock mineral composition and mineral melting rate after Johnson *et al.* (1990) and element distribution coefficient data after McKenzie and O'Nions (1991)

## 5 地幔动力学机制

华北克拉通岩石圈减薄和广泛分布的中、新生代玄武岩一直是研究的热点,其动力学机制更是备受关注。地幔柱模型、断裂模型、热化学侵蚀、岩石圈拆沉都是可能的机制,但也都存在着一定的争议。中国东部的地震波层析成像表明:在中国东部之下的410~660km之间的过渡带内存在水平向西延伸的冷的古太平洋俯冲板片(Kárason and Van der Hilst, 2000; Pei *et al.*, 2004; Zhao, 2004; Zhao *et al.*, 2004),该板片阻止下地幔的热地幔上涌,不利于上地幔内热地幔柱的形成,因此,用地幔柱模型解释中国东部中、新生代火山活动不具有说服力(Niu, 2005)。同时,该冷的板片需要从其上部和下部吸收热量达到热均衡,也没有过剩热量支持热侵蚀作用(Griffin *et al.*, 1998; Menzies and Xu, 1998; 徐义刚,

1999; Xu, 2001; Xu *et al.*, 2004, 2005)。岩石圈拆沉可以较好地解释岩石圈的减薄和新生代玄武岩的地球化学特征(Gao *et al.*, 1998, 2004, 2008, 2009; Xu *et al.*, 2006, 2009, 2010),但是缺少直观的物理理论解释上浮的岩石圈地幔是如何下沉到高密度的软流圈地幔中。拉张断裂和被动上涌减压熔融模型将未知成因的盆地的存在作为中国东部拉张的证据(Davis and Darby, 2010; Wang *et al.*, 2011a, 2012)也是危险的(Niu, 2005)。因此,华北克拉通的岩石圈减薄和中、新生代火山活动的形成机制尚未定论,还需要进一步探讨。

太行山重力梯度带形成于早白垩纪,东西两侧在地貌、地壳厚度、岩石圈厚度、地表热流值均存在明显的差异(Xu, 2007)。太行山重力梯度带的东西两侧陡峭的梯度差异允许我们对重力梯度带附近的新生代玄武岩的成因有新的推测:软流圈由西向东的流动越过重力梯度带时由于岩石圈骤然减薄(岩石圈-软流圈界面从西部的~150km变浅为东部的~80km)必然会发生减压熔融,形成玄武质岩浆(Niu, 2005),断裂的活动与再活化为岩浆的侵入提供了通道,可形成重力梯度带附近广泛分布的新生代火山作用。如果该模型成立,那我们必须思考,什么动力学机制驱动软流圈向东的流动呢?有以下几种观点:

(1)与印度-欧亚板块碰撞有关;印度板块向北俯冲于欧亚板块之下,推挤作用推动鄂尔多斯块体的逆时针旋转,促使太行山地区岩石圈拉张减薄,造成软流圈物质上涌产生玄武岩浆作用(Ren *et al.*, 2002; Zhang *et al.*, 2003; Tang *et al.*, 2006)。此外,印度板块以40mm/y的速度向欧亚板块之下俯冲,>50Ma的连续不断的物质注入必然会驱动软流圈地幔侧向流动(Liu *et al.*, 2004),但是Zhao *et al.* (2011)根据地球物理资料得出太行山地区岩石圈下部的上涌地幔流与印度-欧亚碰撞无关。

(2)与太平洋的向西俯冲有关;地震波层析成像图显示:在中国东部之下410~660km过渡带内存在冷的太平洋俯冲板块,其西端水平延伸至太行山重力梯度带之下(Kárason and Van der Hilst, 2000; Pei *et al.*, 2004; Zhao, 2004; Zhao *et al.*, 2004)。西太平洋俯冲带是全球最大的俯冲带之一,板块向下俯冲,俯冲带上部地幔楔必须有新物质补给,产生“楔吸力”,驱动中国大陆之下的软流圈东流,造成更远的西部软流圈向中国东部之下流动,因为东西岩石圈厚度在重力梯度带处的差异,西部软流圈东流必然会引起减压熔融,形成中国东部的玄武质火山作用(Niu, 2005)。

太行山重力梯度带恰好位于印度-欧亚板块碰撞带和西太平洋俯冲带这两种构造域的边界(Xu, 2007),因此造成这种软流圈东流的驱动力到底是受单一机制的影响还是两种机制的共同作用还需要进一步的研究。

## 6 结论

通过对繁峙玄武岩的元素和同位素地球化学特征的研

究,我们得出以下几点结论:

(1) 繁峙苏孟庄碱性玄武岩和应县亚碱性玄武岩均具有类 OIB 的地球化学特征,与重力梯度带附近的汉诺坝、大同、阳原、集宁、鹤壁等地区新生代玄武岩相似,表明它们可能起源于同一软流圈地幔源区的部分熔融,且存在一定程度的软流圈-岩石圈相互作用。

(2) 岩浆在上升的过程中,地壳混染作用可忽略不计,岩浆演化过程中橄榄石和单斜辉石是常见的分离结晶矿物。

(3) 模拟计算得出苏孟庄碱性玄武岩的熔融程度较小,熔融深度较大;而应县亚碱性玄武岩的熔融程度较大,熔融深度较小。该熔融深度的差异可能受熔融环境和深大断裂的影响。

(4) 重力梯度带附近的新生代的火山活动推测与软流圈的向东流动有关,其驱动力可能是太平洋俯冲板块的楔楔力,也可能是印度板块向欧亚板块的俯冲的物质补给,或者两者兼而有之,该地区广泛分布的断裂带可能为岩浆上涌提供了通道。

**致谢** 野外工作得到了高军平老师、付飘儿、孙文礼的协助;样品分离测试工作得到了文中所提实验室老师及相关人员的极大支持与帮助;审稿人认真阅读了本文,并提出宝贵的修改意见;在此一并表示衷心的感谢!

## References

Bai ZM, Zhang ZJ and Wang YH. 2007. Crustal structure across the Dabie-Sulu orogenic belt revealed by seismic velocity profiles. *Journal of Geophysics and Engineering*, 4(4): 436–442

Barry TL and Kent RW. 1998. Cenozoic magmatism in Mongolia and the origin of Central and East Asian basalts. In: Flower MFJ, Chung SL, Lo CH and Lee TY (eds.). *Mantle Dynamics and Plate Interactions in East Asia*. Geodynamics Series, Vol. 27. Washington DC: American Geophysical Union, 347–364

Basu AR, Wang JW, Huang WK, Xie GH and Tatsumoto M. 1991. Major element, REE, and Pb, Nd, and Sr isotopic geochemistry of Cenozoic volcanic rocks of eastern China: Implications for their origin from suboceanic-type mantle reservoirs. *Earth and Planetary Science Letters*, 105(1–3): 149–169

Chen GY, Song ZH, An CQ *et al.* 1991. Three-dimensional crust and upper mantle structure of the North China region. *Acta Geophysica Sinica*, 34(2): 172–181 (in Chinese with English abstract)

Chi JS and Lu FX. 1996. Kimberlites on the North China Craton and Features of Paleozoic Lithospheric Mantle. Beijing: Science Press (in Chinese)

Choi SH, Mukasa SB, Zhou XH, Xian XH and Andronikov AV. 2008. Mantle dynamics beneath East Asia constrained by Sr, Nd, Pb and Hf isotopic systematics of ultramafic xenoliths and their host basalts from Hannuoba, North China. *Chemical Geology*, 248(1–2): 40–61

Chu ZY, Wu FY, Walker RJ, Rudnick RL, Pitcher L, Puchtel IS, Yang YH and Wilde SA. 2009. Temporal evolution of the lithospheric mantle beneath the eastern North China Craton. *Journal of Petrology*, 50(10): 1857–1898

Davis GA and Darby BJ. 2010. Early cretaceous overprinting of the Mesozoic Daqing Shan fold-and-thrust belt by the Hohhot metamorphic core complex, Inner Mongolia, China. *Geoscience*

*Frontiers*, 1(1): 1–20

Deng JF. 1988. Magma function and deep course of continental rift. In: *Study on Cenozoic Basalts and Upper Mantle in North China*. Beijing: Geological Publishing House, 201–218 (in Chinese)

Deng JF, Zhao HL, Luo ZH, Guo ZF and Mo XX. 1998. Mantle plumes and lithosphere motion in East Asia. In: Flower MFJ, Chung SL, Lo CH, Lee TY (eds.). *Mantle Dynamics and Plate Interactions in East Asia*. Washington DC: American Geophysical Union, 59–65

Deng JF, Mo XX, Zhao HL, Wu ZX, Luo ZH and Su SG. 2004. A new model for the dynamic evolution of Chinese lithosphere: Continental roots-plume tectonics. *Earth-Science Reviews*, 65(3–4): 223–275

DePaolo DJ and Daley EE. 2000. Neodymium isotopes in basalts of the southwest basin and range and lithospheric thinning during continental extension. *Chemical Geology*, 169(1–2): 157–185

Falloon TJ, Green DH, Hatton CJ and Harris KL. 1988. Anhydrous partial melting of a fertile and depleted peridotite from 2 to 30kb and application to basalt petrogenesis. *Journal of Petrology*, 29(6): 1257–1282

Fan QC and Hooper PR. 1991. The Cenozoic basaltic rocks of eastern China: Petrology and chemical composition. *Journal of Petrology*, 32(4): 765–810

Fan WM and Menzies MA. 1992. Destruction of aged lower lithosphere and accretion of asthenosphere mantle beneath eastern China. *Geotectonica et Metallogenia*, 16: 171–181

Fan WM, Zhang HF, Baker J, Jarvis KE, Mason PRD and Menzies MA. 2000. On and off the North China Craton: Where is the Archaean keel? *Journal of Petrology*, 41(7): 933–950

Gao S, Zhang BR, Jin ZM, Kern H, Luo TC and Zhao ZD. 1998. How mafic is the lower continental crust? *Earth and Planetary Science Letters*, 161(1–4): 101–117

Gao S, Rudnick RL, Carlson RW, McDonough WF and Liu YS. 2002. Re-Os evidence for replacement of ancient mantle lithosphere beneath the North China Craton. *Earth and Planetary Science Letters*, 198(3–4): 307–322

Gao S, Rudnick RL, Yuan HL, Liu XM, Liu YS, Xu WL, Ling WL, Ayers J, Wang XC and Wang QH. 2004. Recycling lower continental crust in the North China Craton. *Nature*, 432(7019): 892–897

Gao S, Rudnick RL, Xu WL, Yuan HL, Liu YS, Walker RJ, Puchtel IS, Liu XM, Huang H, Wang XR and Yang J. 2008. Recycling deep cratonic lithosphere and generation of intraplate magmatism in the North China Craton. *Earth and Planetary Science Letters*, 270(1–2): 41–53

Gao S, Zhang JF, Xu WL and Liu YS. 2009. Delamination and destruction of the North China Craton. *Chinese Science Bulletin*, 54(19): 3367–3378

Green DH and O'Hara MJ. 1971. Composition of basaltic magmas as indicators of conditions origin: Application to oceanic volcanism. *Philosophical Transactions of the Royal Society of London (Series A, Mathematical and Physical Sciences)*, 268(1192): 707–725

Griffin WL, Zhang AD, O'Reilly SY and Ryan CG. 1998. Phanerozoic evolution of the lithosphere beneath the Sino-Korean Craton. In: Flower MFJ, Chung SL, Lo CH and Lee TY (eds.). *Mantle Dynamics and Plate Interaction in East Asia*. Washington DC: American Geophysical Union Monograph, 27: 107–126

Griffin WL, O'Reilly SY and Ryan CG. 1999. The composition and origin of sub-continental lithospheric mantle. In: Fei Y, Bertka CM and Mysen BO (eds.). *Mantle Petrology: Field Observations and High-Pressure Experimentation: A Tribute to France R. (Joe) Boyd*. The Geochemical Society Special Publications, 6: 13–46

Griffin WL, O'Reilly SY, Abe N, Aulbach S, Davies RM, Pearson NJ, Doyle BJ and Kivi K. 2003. The origin and evolution of Archean lithospheric mantle. *Precambrian Research*, 127(1–3): 19–41

Guo PY, Niu YL, Ye L, Liu JJ, Sun P, Cui HX, Zhang Y, Gao JP, Su L, Zhao JX and Feng YX. 2014. Lithosphere thinning beneath west North China Craton: Evidence from geochemical and Sr-Nd-Hf isotope compositions of Jining basalts. *Lithos*, 202–203: 27–54

- Hart SR. 1984. A large-scale isotope anomaly in the southern hemisphere mantle. *Nature*, 309(5971): 753–757
- Ho KS, Liu Y, Chen JC, You CF and Yang HJ. 2011. Geochemical characteristics of Cenozoic Jining basalts of the western North China Craton: Evidence for the role of the lower crust, lithosphere, and asthenosphere in petrogenesis. *Terrestrial, Atmospheric and Ocean Sciences*, 22(1): 15–40
- Hofmann AW and White WM. 1982. Mantle plumes from ancient oceanic crust. *Earth and Planetary Science Letters*, 57(2): 421–436
- Huang XL, Zhong JW and Xu YG. 2012. Two tales of the continental lithospheric mantle prior to the destruction of the North China Craton: Insights from Early Cretaceous mafic intrusions in western Shandong, East China. *Geochimica et Cosmochimica Acta*, 96: 193–214
- Jahn BM, Auvray B, Cornichet J, Bai YL, Shenk QH and Liu DY. 1987. 3.5Ga old amphibolites from eastern Hebei Province China: Field occurrence, petrography, Sm-Nd isochron age, and REE geochemistry. *Precambrian Research*, 34(3–4): 311–346
- Jahn BM, Wu FY, Lo CH and Tsai CH. 1999. Crust-mantle interaction induced by deep subduction of the continental crust: Geochemical and Sr-Nd isotopic evidence from post-collisional mafic-ultramafic intrusions of the northern Dabie Complex, Central China. *Chemical Geology*, 157(1–2): 119–146
- Johnson KTM, Dick HJB and Shimizu N. 1990. Melting in the oceanic upper mantle: An ion microprobe study of diopsides in abyssal peridotites. *Journal of Geophysical Research*, 95(B3): 2661–2678
- Káráson H and Van der Hilst RD. 2000. Constraints on mantle convection from seismic tomography. *American Geophysical Union*, 121: 277–288
- Kushiro I. 2001. Partial melting experiments on peridotite and origin of mid-ocean ridge basalt. *Annual Review of Earth and Planetary Sciences*, 29: 71–107
- Lambert IB and Wyllie PJ. 1970. Low-velocity zone of the Earth's mantle: Incipient melting caused by water. *Science*, 169(3947): 764–766
- Langmuir CH, Klein EM and Plank T. 1992. Petrological systematics of mid-ocean ridge basalts: Constraints on melt generation beneath ocean ridges. *Geophysical Monograph-American Geophysical Union*, 71: 183–280
- Li CF, Li XH, Guo JH, Li XH, Li HK, Zhou HY and Li GZ. 2011. Single-step separation of Rb-Sr and Pb from minor rock samples and high precision determination using thermal ionization mass spectrometry. *Geochimica*, 40(5): 399–406 (in Chinese with English abstract)
- Li SG, Xiao TL, Liou DL, Chen YZ, Ge NJ, Zhang ZQ, Sun SS, Cong BL, Zhang RY, Hart SR and Wang SS. 1993. Collision of the North China and Yangtze Blocks and formation of coesite-bearing eclogites: Timing and processes. *Chemical Geology*, 109(1–4): 89–111
- Liu DY, Nutman AP, Compston W, Wu JS and Shen QH. 1992. Remnants of 3800Ma crust in the Chinese part of the Sina-Korean craton. *Geology*, 20(4): 339–342
- Liu M, Cui XJ and Liu FT. 2004. Cenozoic rifting and volcanism in eastern China: A mantle dynamic link to the Indo-Asian collision? *Tectonophysics*, 393(1–4): 29–42
- Liu RX, Chen WJ, Sun JZ and Li DM. 1992. K-Ar chronology and tectonic settings of Cenozoic volcanic rocks in China. In: Liu RX (ed.). *Geochronology and Geochemistry of Cenozoic Volcanic Rocks in China*. Beijing: Seismological Press, 1–43 (in Chinese)
- Ma JL and Xu YG. 2004. Petrology and geochemistry of the Cenozoic basalts from Yangyuan of Hebei Province and Datong of Shanxi Province: Implications for the deep process in the western North China Craton. *Geochimica*, 33(1): 75–88 (in Chinese with English abstract)
- McKenzie D and O'Nions RK. 1983. Mantle reservoirs and ocean island basalts. *Nature*, 301(5897): 229–231
- McKenzie D and O'Nions RK. 1991. Partial melt distributions from inversion of rare earth element concentrations. *Journal of Petrology*, 32(5): 1021–1091
- McKenzie D and O'Nions RK. 1995. The source regions of ocean island basalts. *Journal of Petrology*, 36(1): 133–159
- Meng QR and Zhang GW. 2000. Geologic framework and tectonic evolution of the Qinling orogen, central China. *Tectonophysics*, 323(3–4): 183–196
- Menzies MA, Fan WM and Zhang M. 1993. Palaeozoic and Cenozoic lithoprobes and the loss of >120km of Archaean lithosphere, Sino-Korean Craton, China. Geological Society, London, Special Publications, 76: 71–78
- Menzies MA and Xu YG. 1998. Geodynamics of the North China Craton. In: Flower MFJ, Chung SL, Lo CH and Lee TY (eds.). *Mantle Dynamics and Plate Interactions in East Asia*. Washington DC: American Geophysical Union, 155–165
- Nicholson H and Latin D. 1992. Olivine tholeiites from Krafla Iceland: Evidence for variations in melt fraction within a plume. *Journal of Petrology*, 33(5): 1105–1124
- Niu YL and Batiza R. 1991. An empirical method for calculating melt compositions produced beneath mid-ocean ridges: Application for axis and off-axis (seamounts) melting. *Journal of Geophysical Research*, 96(B13): 21753–21777
- Niu YL, Waggoner DG, Sinton JM and Mahoney JJ. 1996. Mantle source heterogeneity and melting processes beneath seafloor spreading centers: The East Pacific Rise, 18°–19°S. *Journal of Geophysical Research*, 101(B12): 27711–27733
- Niu YL, Bideau D, Hékinian R and Batiza R. 2001. Mantle compositional control on the extent of mantle melting, crust production, gravity anomaly, ridge morphology, and ridge segmentation: A case study at the Mid-Atlantic Ridge 33°–35°N. *Earth and Planetary Science Letters*, 186(3–4): 383–399
- Niu YL and O'Hara MJ. 2003. Origin of ocean island basalts: A new perspective from petrology, geochemistry and mineral physics considerations. *Journal of Geophysical Research*, 108(B4): 2209 (pages ECV 5 1–19)
- Niu YL. 2005. Generation and evolution of basaltic magmas: Some basic concepts and a new view on the origin of Mesozoic-Cenozoic basaltic volcanism in eastern China. *Geological Journal of China Universities*, 11(1): 9–46
- Niu YL. 2008. The origin of alkaline lavas. *Science*, 320(5878): 883–884
- Niu YL, Wilson M, Humphreys ER and O'Hara MJ. 2011. The origin of intra-plate Ocean Island Basalts (OIB): The lid effect and its geodynamic implications. *Journal of Petrology*, 52(7–8): 1443–1468
- Niu YL, Wilson M, Humphreys ER and O'Hara MJ. 2012. A trace element perspective on the source of ocean island basalt (OIB) and fate of subducted ocean crust (soc) and mantle lithosphere (SML). *Episodes*, 35(2): 310–327
- Nohda S, Chen H and Tatsumi Y. 1991. Geochemical stratification in the upper mantle beneath NE China. *Geophysical Research Letters*, 18(1): 97–100
- O'Reilly YS and Griffin WL. 1988. Mantle metasomatism beneath western Victoria, Australia: I. Metasomatic processes in Cr-diopside lherzolites. *Geochimica et Cosmochimica Acta*, 52(2): 433–447
- Pei S, Chen YJ and Zhao DP. 2004. Tomographic structures of East Asia: Data and result. San Francisco: American Geophysical Union Fall Meeting
- Pilet S, Hernandez J, Sylvester P and Poujol M. 2005. The metasomatic alternative for ocean island basalt chemical heterogeneity. *Earth and Planetary Science Letters*, 236(1–2): 148–166
- Ren JY, Tamaki K, Li ST and Zhang JX. 2002. Late Mesozoic and Cenozoic rifting and its dynamic setting in Eastern China and adjacent areas. *Tectonophysics*, 344(3–4): 175–205
- Rudnick RL and Gao S. 2003. Composition of the continental crust. In: Rudnick RL (ed.). *The Crust*. In: Holland HD and Turekian KK (eds.). *Treatise on Geochemistry*, 3: 1–64
- Rudnick RL, Gao S, Yuan HL, Puchtell I and Walker R. 2006. Persistence of Paleoproterozoic lithospheric mantle in the Central

- Zone of the North China Craton. Guangzhou, China; Abstract for the International Conference on Continental Volcanism-lavcel
- Song SG, Su L, Li XH, Zhang GB, Niu YL and Zhang LF. 2010. Tracing the 850Ma continental flood basalts from a piece of subducted continental crust in the North Qaidam UHPM belt, NW China. *Precambrian Research*, 183(4): 805–816
- Song Y, Frey FA and Zhi XC. 1990. Isotopic characteristics of Hannuoba basalts, eastern China; Implications for their petrogenesis and the composition of subcontinental mantle. *Chemical Geology*, 88(1–2): 35–52
- Sun SS and McDonough WF. 1989. Chemical and isotopic systematics of oceanic basalts; Implications for mantle composition and processes. In: Saunders AD and Norry MJ (eds.). *Magmatism in the Ocean Basins*. Geological Society, London, Special Publications, 42(1): 313–345
- Tang YJ, Zhang HF and Ying JF. 2004. High-Mg olivine xenocrysts entrained in Cenozoic basalts in central Taihang Mountains; Relicts of old lithospheric mantle. *Acta Petrologica Sinica*, 20(5): 1243–1252 (in Chinese with English abstract)
- Tang YJ, Zhang HF and Ying JF. 2006. Asthenosphere-lithospheric mantle interaction in an extensional regime; Implication from the geochemistry of Cenozoic basalts from Taihang Mountains, North China Craton. *Chemical Geology*, 233(3–4): 309–327
- Tang YJ, Zhang HF, Ying JF, Su BX, Chu ZY, Xiao Y and Zhao XM. 2012. Highly heterogeneous lithospheric mantle beneath the Central Zone of the North China Craton evolved from Archean mantle through diverse melt refertilization. *Gondwana Research*, 23(1): 130–140
- Tatsumoto M, Basu AR, Huang WK, Wang JW and Xie GH. 1992. Sr, Nd, Pb isotopes of ultramafic xenoliths in volcanic rocks of East China; Enriched components EM I and EM II in subcontinental lithosphere. *Earth and Planetary Science Letters*, 113(1–2): 107–128
- Vervoort JD and Blichert-Toft J. 1999. Evolution of the depleted mantle: Hf isotope evidence from juvenile rocks through time. *Geochimica et Cosmochimica Acta*, 63(3–4): 533–556
- Wang HF, Yang XC, Zhu BG, Fan SK and Dai TM. 1988. K-Ar geochronology and evolution of Cenozoic volcanic rocks in eastern China. *Geochimica*, 17(1): 1–12 (in Chinese with English abstract)
- Wang T, Zheng YD, Zhang JJ, Zeng LS, Donskaya T, Guo L and Li JB. 2011a. Pattern and kinematic polarity of Late Mesozoic extension in continental NE Asia; Perspectives from metamorphic core complexes. *Tectonics*, 30(6): TC6007
- Wang T, Guo L, Zheng YD, Donskaya T, Gladkochub D, Zeng LS, Li JB, Wang YB and Mazukabzov A. 2012. Timing and processes of Late Mesozoic mid-lower-crustal extension in continental NE Asia and implications for the tectonic setting of the destruction of the North China Craton; Mainly constrained by zircon U-Pb ages from metamorphic core complexes. *Lithos*, 154: 315–345
- Wang Y, Zhao ZF, Zheng YF and Zhang JJ. 2011b. Geochemical constraints on the nature of mantle source for Cenozoic continental basalts in east-central China. *Lithos*, 125(3–4): 940–955
- Wang YJ, Fan WM, Zhang HF and Peng TP. 2006. Early Cretaceous gabbroic rocks from the Taihang Mountains; Implications for a paleosubduction-related lithospheric mantle beneath the central North China Craton. *Lithos*, 86(3–4): 281–302
- Weaver BL. 1991. The origin of ocean island basalt end-member compositions: Trace element and isotopic constraints. *Earth and Planetary Science Letters*, 104(2–4): 381–397
- White WM and Duncan RA. 1996. Geochemistry and geochronology of the Society Islands; New evidence for deep mantle recycling. *American Geophysical Union Geophysical Monograph*, 95: 183–206
- Windley BF, Alexeiev D, Xiao W, Kröner A and Badarch G. 2007. Tectonic models for accretion of the Central Asian Orogenic Belt. *Journal of the Geological Society*, 164(1): 31–47
- Wu FY, Walker RJ, Ren XW, Sun DY and Zhou XH. 2003. Osmium isotopic constraints on the age of lithospheric mantle beneath northeastern China. *Chemical Geology*, 196(1–4): 107–129
- Wu FY, Ge WC, Sun DY and Guo CL. 2003. Discussions on the lithospheric thinning in eastern China. *Earth Science Frontiers*, 10(3): 51–60 (in Chinese with English abstract)
- Wu FY, Walker RJ, Yang YH, Yuan HL and Yang JH. 2006. The chemical-temporal evolution of lithospheric mantle underlying the North China Craton. *Geochimica et Cosmochimica Acta*, 70(19): 5013–5034
- Xie GH and Wang JW. 1992. The geochemistry of Hannuoba basalts and their ultra-mafic xenoliths. In: Liu RX (ed.). *The Age and Geochemistry of Cenozoic Volcanic Rock in China*. Beijing: Seismological Press, 149–170 (in Chinese)
- Xu WL, Wang QH, Wang DY, Guo JH and Pei FP. 2006. Mesozoic adakitic rocks from the Xuzhou-Suzhou area, eastern China; Evidence for partial melting of delaminated lower continental crust. *Journal of Asian Earth Sciences*, 27(4): 454–464
- Xu WL, Gao S, Yang DB, Pei FP and Wang QH. 2009. Geochemistry of eclogite xenoliths in Mesozoic adakitic rocks from Xuzhou-Suzhou area in central China and their tectonic implications. *Lithos*, 107(3–4): 269–280
- Xu WL, Yang DB, Gao S, Pei FP and Yu Y. 2010. Geochemistry of peridotite xenoliths in Early Cretaceous high-Mg<sup>#</sup> diorites from the Central Orogenic Block of the North China Craton; The nature of Mesozoic lithospheric mantle and constraints on lithospheric thinning. *Chemical Geology*, 270(1–4): 257–273
- Xu YG. 1999. Roles of thermo-mechanic and chemical erosion in continental lithospheric thinning. *Bulletin of Mineralogy Petrology and Geochemistry*, 18(1): 1–5 (in Chinese with English abstract)
- Xu YG. 2001. Thermo-tectonic destruction of the Archean lithospheric keel beneath the Sino-Korean Craton in China; Evidence, timing and mechanism. *Physics and Chemistry of the Earth, Part A: Solid Earth and Geodesy*, 26(9–10): 747–757
- Xu YG, Chung SL, Ma JL and Shi LB. 2004. Contrasting Cenozoic lithospheric evolution and architecture in the Western and Eastern Sino-Korean Craton; Constraints from geochemistry of basalts and mantle xenoliths. *The Journal of Geology*, 112(5): 593–605
- Xu YG, Ma JL, Frey FA, Feigenson MD and Liu JF. 2005. Role of lithosphere-asthenosphere interaction in the genesis of Quaternary alkali and tholeiitic basalts from Datong, western North China Craton. *Chemical Geology*, 224(4): 247–271
- Xu YG. 2006a. Formation of the Taihangshan gravity lineament by the diachronous lithospheric thinning of the North China craton. *Earth Science*, 31(1): 14–22 (in Chinese with English abstract)
- Xu YG. 2006b. Using basalts geochemistry to constrain Mesozoic-Cenozoic evolution of the lithosphere beneath North China Craton. *Earth Science Frontiers*, 13(2): 93–104 (in Chinese with English abstract)
- Xu YG. 2007. Diachronous lithospheric thinning of the North China Craton and formation of the Daxin'anling-Taihangshan gravity lineament. *Lithos*, 96(1–2): 281–298
- Ye H, Zhang BT and Mao FY. 1987. The Cenozoic tectonic evolution of the great North China; Two types of rifting and crustal necking in the great North China and their tectonic implications. *Tectonophysics*, 133(3–4): 217–227
- Zhang HF, Sun M, Zhou XH, Fan WM, Zhai MG and Yin JF. 2002. Mesozoic lithosphere destruction beneath the North China Craton; Evidence from major, trace-element and Sr-Nd-Pb isotope studies of Fangcheng basalts. *Contributions to Mineralogy and Petrology*, 144(2): 241–254
- Zhang HF, Min S, Zhou MF, Fan WM, Zhou XH and Zhai MG. 2004. Highly heterogeneous Late Mesozoic lithospheric mantle beneath the North China Craton; Evidence from Sr-Nd-Pb isotopic systematics of mafic igneous rocks. *Geological Magazine*, 141(1): 55–62
- Zhang JJ, Zheng YF and Zhao ZF. 2009. Geochemical evidence for interaction between oceanic crust and lithospheric mantle in the origin of Cenozoic continental basalts in east-central China. *Lithos*, 110(1–4): 305–326
- Zhang M, Zhou XH and Zhang JB. 1998. Nature of the lithospheric

- mantle beneath NE China: Evidence from potassic volcanic rocks and mantle xenoliths. In: Flower MFJ, Chung SL, Lo CH and Lee TY (eds.). *Mantle Dynamics and Plate Interactions in East Asia*. Geodynamics Series, American Geophysical Union, Washington, 197-219
- Zhang M, Yang JH, Sun JF, Wu FY and Zhang M. 2012a. Juvenile subcontinental lithospheric mantle beneath the eastern part of the Central Asian Orogenic Belt. *Chemical Geology*, 328: 109-122
- Zhang WH, Han BF, Du W and Liu ZQ. 2005. Characteristics of mantle source for Jining Cenozoic basalts from southern Inner Mongolia: Evidence from element and Sr-Nd-Pb isotopic geochemistry. *Acta Petrologica Sinica*, 21(6): 1569-1582 (in Chinese with English abstract)
- Zhang WH, Zhang HF, Fan WM, Han BF and Zhou MF. 2012b. The genesis of Cenozoic basalts from the Jining area, northern China: Sr-Nd-Pb-Hf isotope evidence. *Journal of Asian Earth Sciences*, 61: 128-142
- Zhang YQ, Ma YS, Yang N, Shi W and Dong SW. 2003. Cenozoic extensional stress evolution in North China. *Journal of Geodynamics*, 36(5): 591-613
- Zhao DP. 2004. Global tomographic images of mantle plumes and subducting slabs: Insight into deep Earth dynamics. *Physics of the Earth and Planetary Interiors*, 146(1-2): 3-34
- Zhao DP, Lei JS and Tang RY. 2004. Origin of the Changbai intraplate volcanism in Northeast China: Evidence from seismic tomography. *Chinese Science Bulletin*, 49(13): 1401-1408
- Zhao GC, Wilde SA, Cawood PA and Lu LZ. 1999. Tectonothermal history of the basement rocks in the western zone of the North China Craton and its tectonic implications. *Tectonophysics*, 310(1-4): 37-53
- Zhao GC, Wilde SA, Cawood PA and Sun M. 2001. Archean blocks and their boundaries in the North China Craton: Lithological geochemical structural and *P-T* path constraints and tectonic evolution. *Precambrian Research*, 107(1-2): 45-73
- Zhao L, Zheng TY, Lu G and Ai YS. 2011. No direct correlation of mantle flow beneath the North China Craton to the India-Eurasia Collision: Constraints from new SKS wave splitting measurements. *Geophysical Journal International*, 187(2): 1027-1037
- Zhao ZF and Zheng YF. 2009. Remelting of subducted continental lithosphere: Petrogenesis of Mesozoic magmatic rocks in the Dabie-Sulu orogenic belt. *Science in China (Series D)*, 52(9): 1295-1318
- Zheng JP. 1999. *Mesozoic-Cenozoic Mantle Replacement and Lithospheric Thinning beneath the Eastern China*. Wuhan: China University of Geosciences Press (in Chinese)
- Zheng JP, O'Reilly SY, Griffin WL, Lu FX, Zhang M and Pearson NJ. 2001. Relict refractory mantle beneath the eastern North China block: Significance for lithosphere evolution. *Lithos*, 57(1): 43-66
- Zheng JP, Griffin WL, O'Reilly SY, Yu CM, Zhang HF, Pearson N and Zhang M. 2007. Mechanism and timing of lithospheric modification and replacement beneath the eastern North China Craton: Peridotitic xenoliths from the 100Ma Fuxin basalts and a regional synthesis. *Geochimica et Cosmochimica Acta*, 71(21): 5203-5225
- Zheng JP, Griffin WL, Qi L, O'Reilly SY, Sun M, Zheng S, Pearson N, Gao JF, Yu CM, Su YP, Tang HY, Liu QS and Wu XL. 2009. Age and composition of granulite and pyroxenite xenoliths in Hannuoba basalts reflect Paleogene underplating beneath the North China Craton. *Chemical Geology*, 264(1-4): 266-280
- Zheng YF, Xiao WJ and Zhao GC. 2013. Introduction to tectonics of China. *Gondwana Research*, 23(4): 1189-1206
- Zhi XC, Song Y, Frey FA, Feng JL and Zhai MZ. 1990. Geochemistry of Hannuoba basalts, eastern China: Constraints on the origin of continental alkalic and tholeiitic basalt. *Chemical Geology*, 88(1-2): 1-33
- Zhou XH and Armstrong RL. 1982. Cenozoic volcanic rocks of eastern China: Secular and geographic trends in chemistry and strontium isotopic composition. *Earth and Planetary Science Letters*, 58(3): 301-329
- Zhu YS, Hou GS and Yang JH. 2012. Sources and petrogenesis of the Cenozoic alkali basalts in Hebi, eastern North China Craton: Geochemical and Sr-Nd-Hf isotopic evidence. *Acta Petrologica Sinica*, 28(12): 4064-4076 (in Chinese with English abstract)
- Zindler A and Hart S. 1986. Chemical geodynamics. *Annual Review of Earth and Planetary Sciences*, 14: 493-571
- Zou HB, Zindler A, Xu XS and Qi Q. 2000. Major, trace element, and Nd, Sr and Pb isotope studies of Cenozoic basalts in SE China: Mantle sources, regional variations, and tectonic significance. *Chemical Geology*, 171(1-2): 33-47
- Zou HB, Reid MR, Liu YS, Yao YP, Xu XS and Fan QC. 2003. Constraints on the origin of historic potassic basalts from northeast China by U-Th disequilibrium data. *Chemical Geology*, 200(1-2): 189-201

### 附中文参考文献

- 陈国英, 宋仲和, 安昌强等. 1991. 华北地区三维地壳上地幔结构. *地球物理学报*, 34(2): 172-181
- 池际尚, 路凤香. 1996. 华北地台金伯利岩及古生代岩石圈地幔特征. 北京: 科学出版社
- 邓晋福. 1988. 大陆裂谷岩浆作用及深部过程. 见: 中国东部新生代玄武岩及上地幔研究. 北京: 地质出版社, 201-218
- 李潮峰, 李献华, 郭敬辉, 李向辉, 李怀坤, 周红英, 李国占. 2011. 微量岩石样品中 Rb-Sr 和 Pb 一步分离及高精度热电离子质谱测试. *地球化学*, 40(5): 399-406
- 刘若新, 陈文寄, 孙建中, 李大明. 1992. 中国新生代火山岩的 K-Ar 年代与构造环境. 见: 刘若新主编. 中国新生代火山岩年代学与地球化学. 北京: 地震出版社, 1-43
- 马金龙, 徐义刚. 2004. 河北阳原和山西大同新生代玄武岩的岩石地球化学特征: 华北克拉通西部深部地质过程初探. *地球化学*, 33(1): 75-88
- 汤艳杰, 张宏福, 英基丰. 2004. 太行山中段新生代玄武岩中高镁橄榄石捕虏晶: 残留古老岩石圈地幔样品. *岩石学报*, 20(5): 1243-1252
- 王慧芬, 杨学昌, 朱炳泉, 范嗣昆, 戴植谟. 1988. 中国东部新生代火山岩 K-Ar 年代学及其演化. *地球化学*, 17(1): 1-12
- 吴福元, 葛文春, 孙德有, 郭春丽. 2003. 中国东部岩石圈减薄研究中的几个问题. *地学前缘*, 10(3): 51-60
- 解广轰, 王俊文. 1992. 汉诺坝玄武岩及其超镁铁岩捕虏体的地球化学. 见: 刘若新主编. 中国新生代火山岩年代学与地球化学. 北京: 地震出版社, 149-170
- 徐义刚. 1999. 岩石圈的热-机械侵蚀和化学侵蚀与岩石圈减薄. *矿物岩石地球化学通报*, 18(1): 1-5
- 徐义刚. 2006a. 太行山重力梯度带的形成与华北岩石圈减薄的时空差异性有关. *地球科学*, 31(1): 14-22
- 徐义刚. 2006b. 用玄武岩组成反演中-新生代华北岩石圈的演化. *地学前缘*, 13(2): 93-104
- 张文慧, 韩宝福, 杜蔚, 刘志强. 2005. 内蒙古集宁新生代玄武岩的地幔源区特征: 元素及 Sr-Nd-Pb 同位素地球化学证据. *岩石学报*, 21(6): 1569-1582
- 郑建平. 1999. 中国东部地幔置换作用与中生代岩石圈减薄. 武汉: 中国地质大学出版社
- 朱昱升, 侯广顺, 杨进辉. 2012. 鹤壁新生代玄武岩源区及成因: 地球化学和 Sr-Nd-Hf 同位素证据. *岩石学报*, 28(12): 4064-4076